Journal of Environmental Management 372 (2024) 123406

Contents lists available at ScienceDirect

Journal of Environmental Management

journal homepage: www.elsevier.com/locate/jenvman

Research article

Effectiveness of ozone nanobubble treatments on high biomass cyanobacterial blooms: A mesocosm experiment and field trial

Justin D. Chaffin [a,*], David E. Berthold [b], Eugene C. Braig [c], Josh D. Fuchs [d], Rachel S. Gabor [e], Stephen J. Jacquemin [f], Haley E. Kuhn [d], Lillian D. Labus [e], H. Dail Laughinghouse [b], Forrest W. Lefler [b], Heath E. Mash [g], Heather A. Raymond [h], Holly Stanley [e], Autumn T. Taylor [a,b], Linda K. Weavers [d], Skye Wendel [f]

[a] F.T. Stone Laboratory and Ohio Sea Grant, The Ohio State University, 878 Bayview Ave. P.O. Box 119, Put-In-Bay, OH 43456, USA
[b] Agronomy Department, Fort Lauderdale Research and Education Center, University of Florida—IFAS, 3205 College Avenue, Davie, FL 33314, USA
[c] Ohio State University Extension, School of Environment and Natural Resources, 2021 Coffey Rd., Columbus, OH 43210, USA
[d] Civil, Environmental and Geodetic Engineering and Ohio Water Resources Center, The Ohio State University, 2070 Neil Ave., Columbus, OH 43210, USA
[e] School of Environment and Natural Resources, The Ohio State University, 2021 Coffey Rd, Columbus, OH 43210, USA
[f] Agriculture and Water Quality Education Center, Wright State University - Lake Campus, Celina, OH 45822, USA
[g] Center for Environmental Solutions and Emergency Response, Office of Research and Development, United States Environmental Protection Agency, 26 W. Martin Luther King Dr., Cincinnati, OH 45268, USA
[h] Office of Research and Graduate Education, College of Food, Agricultural, and Environmental Sciences, The Ohio State University, 2120 Fyffe Rd, Columbus, OH 43210, USA

ARTICLE INFO

Keywords:
CyanoHABs
Control strategies
Eutrophication
Grand lake St Marys
Microcystin
Nanobubble ozone treatment
Planktothrix

ABSTRACT

Cyanobacterial harmful algae blooms (cyanoHABs) are a global threat to water resources, and lake managers need effective strategies to suppress or control them. Algaecides may have negative environmental impacts, and their use is becoming restricted. Nanobubble ozone technology (NBOT) is an emerging water treatment option with potentially fewer negative impacts. We assessed the effectiveness of NBOT in treating *Planktothrix* cyanoHAB from Grand Lake St Marys (GLSM, Ohio USA) in a mesocosm (2,000L) experiment and two 4-week trials in a GLSM embayment (Sunset Beach, SBE; ~$4.7*10^7$ L). In mesocosms, the medium (1.21 ± 0.08 ozone to dissolved organic carbon ratio, O_3:DOC) and high (2.04 ± 0.07 O_3:DOC) doses decreased both chlorophyll *a* (chl-*a*) and phycocyanin by 98–99% and microcystins by 62% and 92%, respectively. The low dose (0.68 ± 0.05 O_3:DOC) decreased chl-*a* and phycocyanin by over 70%. No effect was observed for chl-*a* nor microcystins in both oxygen-only nanobubble mesocosm treatments and the SBE NBOT trial. The average O_3:DOC at SBE was less than the low NBOT mesocosm experiment dose, and the percentage of water treated was lower. DOC chemistry, as indicated by $SUVA_{254}$, was more oxidized at the NBOT outlet than the inlet in the SBE trial, suggesting interaction with ozone. However, no differences were observed 3m from the outlet, indicating minimal treatment reach. The mesocosm experiment highlighted NBOT's ability to control cyanoHABs, but the limited effectiveness of NBOT at SBE was likely due to high cyanobacteria biomass and DOC at the onset of treatment, low O_3:DOC, and low percentage of lake water instantaneously treated.

1. Introduction

Freshwater cyanobacterial harmful algal blooms (cyanoHABs) have become a worldwide issue because of a warming climate and anthropogenic nutrient sources from humans (e.g. poor sewage treatment and heavy fertilizer applications) that increase the delivery of growth-stimulating nutrients (phosphorus and nitrogen) leading to eutrophication (O'Neil et al., 2012; Paerl and Huisman, 2008; Zepernick et al., 2023). Many cyanobacterial species produce toxins, often called "cyanotoxins," that have harmful effects on humans and wildlife (Carmichael, 1992; Carmichael and Boyer, 2016). CyanoHABs affect sources of drinking (Qin et al., 2010; Steffen et al., 2017) and recreational waters (World Health Organization, 2020), and cyanotoxins may become aerosolized (Plaas and Paerl, 2021; Shi et al., 2023).

* Corresponding author.
E-mail address: chaffin.46@osu.edu (J.D. Chaffin).

https://doi.org/10.1016/j.jenvman.2024.123406
Received 6 August 2024; Received in revised form 14 October 2024; Accepted 15 November 2024
Available online 22 November 2024

Additionally, the high biomasses of blooms negatively affect aquatic ecosystems (Backer et al., 2013; Tillmanns et al., 2008) and local economies (Dodds et al., 2009; Smith et al., 2019; Wolf et al., 2022). Therefore, to protect human health and ecological integrity, we must investigate methods to combat cyanoHABs.

The ideal method to deal with cyanobacterial blooms is prevention by minimizing external nutrient loads into waterways (Kibuye et al., 2021). However, many lakes continue to have high external nutrient loading from point and non-point sources that are often difficult to control. For example, agricultural fields often have a buildup of legacy phosphorus (Osterholz et al., 2020) and it may take years to decades for lakes to realize improvements in water quality following nutrient abatement practices (Jeppesen et al., 2005). Even if external loads can be greatly reduced, after decades of excessive anthropogenic nutrient loading lake bottom sediments often become nutrient-rich and recycle nutrients between the sediments and water column, continuing to fuel cyanobacterial blooms even after external loads are reduced (Søndergaard et al., 2003). Therefore, in search of quicker solutions, many lake managers opt for algaecides (copper or hydrogen peroxide based) to treat algae and flocculants (e.g., alum or lanthanum) to bind phosphorus in the water column and inhibit phosphorus release from lake sediments (Kibuye et al., 2021; Osgood et al., 2017). However, chemical-based treatment options have significant disadvantages to their use such as affecting non-target algae and organisms (e.g., zooplankton and fish kills), altering pH, accumulation of metals in the lake sediments, and the need for repeated applications (Kibuye et al., 2021). Moreover, many authorities are banning and discouraging algaecides like copper sulfate (Burford et al., 2019); therefore, other options should be explored to control blooms.

Nanobubble ozone technology (NBOT) is an emerging technology with the potential to control cyanoHABs while reducing the putative negative factors associated with traditional control strategies (Atkinson et al., 2019; Batagoda et al., 2019). Ozone has been used since the early 1900s to treat drinking water and wastewater (Lee et al., 2013), including -more recently-treatment for microcystins (He et al., 2016; Rositano et al., 1998). Compared to macrobubbles, the buoyancy force of nanobubbles is small, which results in bubbles persisting in the water column for longer periods of time. Additionally, nanobubbles have a strong surface charge which is speculated to decrease the diffusion rate of ozone from the gaseous bubble (Meegoda et al., 2019). Therefore, by incorporating ozone into nanobubbles, it is not released from the water to the air during treatment and may persist for a longer time (Soyluoglu et al., 2023). In aquaculture, NBOT has been shown to decrease heterotrophic bacteria abundances while not impacting fish (Huang et al., 2023; Jhunkeaw et al., 2021; Thanh Dien et al., 2021). While NBOT shows promise for treatment of bacterial infections in aquaculture, the application of NBOT to lakes for cyanoHAB mitigation is novel and an assessment of NBOT for the treatment of cyanoHABs is needed. In drinking water and wastewater treatment, the degradation of micropollutants or viruses by ozone can be predicted by the mass ratio of the ozone to dissolved organic carbon dose (mg of O_3 to mg C of DOC, O_3:DOC) with higher amounts of ozone required as the DOC increases (Czekalski et al., 2016; Lee et al., 2013; Wolf et al., 2019). However, ozone decay rate increases by roughly an order of magnitude per pH unit above pH 8 (Gardoni et al., 2012), and cyanobacterial blooms often create high pH (Verspagen et al., 2014). One limitation of ozone use in drinking water systems is the potential formation of bromate, which can be a concern if source water bromide concentrations exceed 50 μg L^{-1} and pH is elevated (Morrison et al., 2023; Rakness, 2011; von Gunten and Pinkernell, 2000).

The objective of this study was to evaluate the effectiveness of NBOT at treating a high biomass cyanoHAB. Grand Lake St. Marys (GLSM), Ohio, USA, is one of the most hypereutrophic lakes in North America (Mishra et al., 2019). GLSM is a large (89 km^2), shallow (average depth 1.5–2.0 m), human-made canal-feeder lake with persistent cyanoHABs dominated by *Planktothrix argardhii* and year-around microcystin detections that frequently exceed recreational guideline concentrations of 8 μg L^{-1} (Filbrun et al., 2013; Jacquemin et al., 2018, 2023b). Utilizing a GLSM sourced cyanoHAB, NBOT treatment was assessed based on affects to total phytoplankton biomass (measured as chlorophyll *a* concentration), total concentration of microcystins and the phase of the toxins (intracellular vs. extracellular), microbial community structure, DOC concentration, and cell viability. A mesocosm study tested the effectiveness of NBOT at different dosing levels in a small-scale, highly-controlled environment and a field trial tested the effectiveness of NBOT and zone of influence of treatment in-situ at the lake scale. In both studies, the O_3:DOC ratio and how it impacted treatment was evaluated, in order to be consistent with how ozone is used in water and wastewater treatment plants (Lee et al., 2013).

2. Material and methods

2.1. NanoBubble ozone treatment (NBOT) units

Ozone nanobubbles were generated using NBOT units provided by Green Water Solutions, LLC (Brookfield, Ohio, USA). First, an Onyx Ultra PSA Oxygen Generator (AirSep Corporation, Buffalo, New York, USA) creates a dry oxygen feed gas to Atlas 30 ozone generator(s) (Absolute Ozone, Edmonton, AB, Canada). The gaseous ozone concentration was monitored using a Model 106-L Ozone Monitor (2B Technologies, Broomfield, Colorado, USA). The ozone gas is infused into the reacting solution via a venturi injector. Then, effluent ozonated water flows into an internal contact tank equipped with a gaseous ozone destruct unit to eliminate any released gaseous ozone. Water is pumped through the NBOT unit under constant pressure through a patented nozzle that breaks larger bubbles into smaller nanobubbles. An ozone sensor with alarm was used to monitor ambient ozone. Also, the unit was equipped with emergency shut-offs in the event of an ozone leak or equipment failure.

2.2. Mesocosm experiment

GLSM water (~13,000 L) was hauled to Ohio State University's Stone Lab with three Ohio Division of Wildlife fish-hatchery trucks on July 26, 2023. The mesocosm facility at Stone Laboratory has 15 2200-L tanks (1.8 m diameter, 0.91 m deep in the center of the tank, 0.86 m deep on the edge of the tank). Each tank was filled with GLSM water (40%) and filtered (1 μm) Lake Erie water (60%) with the mesocosm facilities pumps and filters. To prevent nutrient limitation, sodium phosphate dibasic and sodium nitrate were added to the tanks to increase concentrations by 5 and 100 μmol L^{-1}, respectively. The tanks were covered with a screen that reduced surface sunlight by 55%. Tanks were exposed to natural sunlight (i.e., no artificial lights) and ambient temperature (no temperature control) throughout the initial incubation and the experiment. The algae incubated for 3 days before the experiment began, and the tanks were stirred and aerated twice a day. Initial samples (hour 0) were collected from all 15 tanks on July 30, 2023 before NBOT treatment began. Three tanks that did not receive NBOT served as control. Three other tanks served as oxygen-only nanobubble controls in which lake water passed through the NBOT unit pump, but the ozone generators were not on. The three NBOT ozone dosage treatments were 4.9 ± 0.4 mg O_3 L^{-1} (mean ± 1 standard error) ("low"), 8.9 ± 0.4 mg O_3 L^{-1} ("medium") and 14.9 ± 0.4 mg O_3 L^{-1} ("high") and each dosage was replicated with three tanks. In all treatment tanks, 100% of the water passed through the NBOT unit. To confirm and quantify ozone generated by the NBOT units, we measured the flow rate and gas phase ozone.

Samples from the tanks were collected prior to treatment and at 1, 4, 8, 24, 48, 72, and 96 h after treatment. The tanks were aerated throughout the experiment and thoroughly mixed prior (minutes) to grab sample collection and data recording to ensure a homogenous water column. A Yellow Springs Instruments (YSI) EXO2 multi-

parameter sonde was used to collect data on cyanobacteria biomass, measured as phycocyanin relative fluorescence, at each time point. Grab samples from the tanks were collected with four equal-volume subsamples (one each from the four cardinal directions) with a 1-m-long integrated tube sampler and deposited and mixed into a clean bucket which had been rinsed with sample water. For chlorophyll (chl) *a* concentrations, ~2 L of water was poured into 2.4-L dark polycarbonate bottles and placed in a cooler with ice for immediate delivery to the laboratory (adjacent to mesocosm facility). Samples for cell viability and microscopy were taken from the 2.4-L dark bottle. For total microcystins (MCs), ~25 mL of water was poured into 60-mL amber glass vials and placed in a cooler on ice. For extracellular microcystins, 60-mL polyethylene terephthalate glycol (PETG) bottles were rinsed three times with filtered lake water (0.7 μm glass fiber filter syringe filter; which also rinsed the filter) and then 40 mL of additional filtered lake water was saved in the PETG bottle and placed on ice. For dissolved organic carbon (DOC), 40-mL pre-combusted amber glass vials were rinsed three times with sample water filtered with 0.2-μm PES syringe filters and then filled without air space. Analytical methods are provided in the following section.

2.3. In situ lake trial

The in-situ NBOT trial at GLSM took place in a small artificial embayment, called the Sunset Beach Enclosure (SBE; also known as Dog Tale Lake), that is isolated from the main lake by the construction of two break walls that partially encircle SBE (Fig. 1). SBE has an area of ~3.2 $\times 10^4$ m^2, an average depth of ~1.5 m, and an estimated volume of 4.8 $\times 10^4$ m^3. NBOT units were deployed for two 4-week periods that were separated by a 4-week period without NBOT treatment during summer 2023 (NBOTs on 12 June to 10 July and 7 August to 4 September). Two NBOT units were deployed at the east and west ends of SBE where the beach and break walls intersect (Fig. 1). Given the pump rate of the NBOT units (4.1 x 10^5 L d^{-1} per NBOT; 8.2 x 10^5 L d^{-1} total for both NBOT units) and assuming perfect circulation and no water exchange from the main lake, only 1.7% and 48% of the SBE (~4.8 x 10^7 L) could be directly treated during a 24-h period and during each 4-week trial, respectively. Each NBOT unit had four ozone generators, and the total ozone load to SBE was determined as the sum of ozone from each ozone generator. To confirm and quantify ozone generated by the NBOT units, we measured the flow rate and gas phase ozone on seven dates during the 2023 SBE trial (14 June, 27 June, 5 July, 8 August, 16 August, 22 August, 29 August). The two NBOTs generated a combined average of 0.21 kg of ozone per hour (5.1 O_3 kg d^{-1}) with a flow rate of 3.4 x 10^4 L per hour (8.2 x 10^5 L d^{-1}), or 6.31 mg O_3 L^{-1} in the outlet.

Initial water samples were collected on May 31, 2023 and then weekly from June 6, 2023 to September 19, 2023 from 15 total locations (Fig. 1). Samples were collected near the NBOT inlets, from the NBOT outlet hose, and 3.3 m, 10 m, 33 m, and 100 m from the NBOT outlet (the 100-m sample was the mid-point between the two NBOT units). The samples were collected by wading to hip-depth water. Water was collected at elbow depth using a Nalgene bottle to fill a clean and lake-water-rinsed 20-L bucket. The NBOT outlet samples were collected only when the NBOTs were deployed. The NBOT inlet samples were collected weekly near the NBOT inlet when NBOTs were deployed and where the inlets were when NBOTs were not deployed. Control site samples were collected in the main lake from the breakwall adjacent to the NBOT units and in the main lake outside of the curtain that partially separates SBE from the main lake. Samples from the break wall were collected by using a Nalgene bottle attached to a sampling stick to collect water just beneath the surface and poured into the bucket. An additional sample was collected in SBE inside the curtain from the break wall. Sample buckets with water were carried to the beach and sample processing began immediately as stated in the mesocosm experiment section, except DOC samples were filtered with pre-combusted 47-mm, 0.7-μm GFF filters. Additionally, samples for total nitrogen and total phosphorus were stored in 250-mL PETG bottles, and the filtered samples were analyzed for dissolved reactive phosphate, nitrate and nitrite, and ammonium. Samples were transported to the laboratory on ice and further processing occurred within 6 h of sample collection.

Additionally, a YSI EXO2 multi-parameter sonde was attached to a YSI DB600 buoy deployed in the center of SBE (~100 m from the east

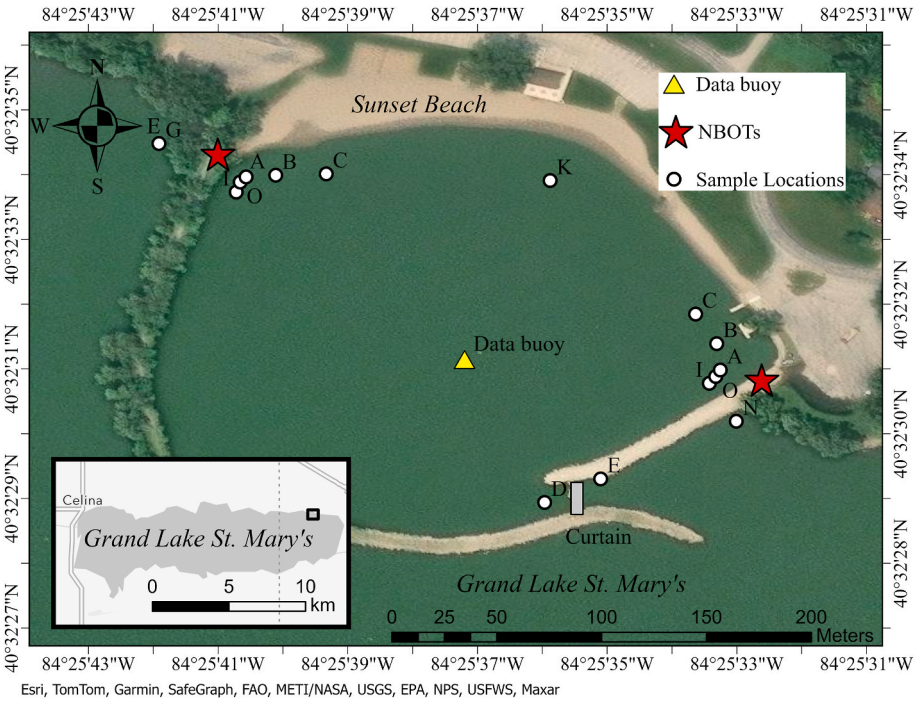

Fig. 1. Sample locations in the Sunset Beach Enclosure during 2023 (circles), the nanobubble ozone generators (stars) location, and the data buoy (triangle). I = inlets, O = outlet, A, B, C, and K are 3, 10, 30, and 110 m from the NBOT outlets. The NBOT inlets were facing to the south and parallel with the breakwalls, and the NBOT outlets faced the beaches. Sunset Beach enclosure is in the northeast corner of Grand Lake St. Mary's, as shown in the inset figure.

NBOT and ~130 m from the west NBOT; Fig. 1). The sonde recorded water temperature, pH, turbidity (Formazin Nephelometric Units, FNU), dissolved oxygen (mg L^{-1} and temperature-corrected percent saturation), phycocyanin fluorescence (relative fluorescence units, RFU), chl fluorescence (RFU), and fluorescent dissolved organic matter (fDOM, RFU) at 15-min intervals.

2.4. Analytical methods

2.4.1. Chlorophyll

Three metrics were used to quantify total phytoplankton and cyanobacteria biomass specifically: 1) filter-extracted chl *a* concentration, 2) a FluoroProbe, which determines the amount of chl *a* associated with green algae, diatoms, cyanobacteria, and cryptophytes, and 3) a YSI EXO2 sonde equipped with the total algae sensor the measures chl and phycocyanin RFU. For filter-extracted chl *a* concentrations, 250–400 mL, depending on phytoplankton biomass, was filtered onto a 47-mm glass fiber filter (GF/F; 0.7 nominal pore size, Cytiva, 1,825,047). The filters were stored on silica gel in mini-petri dishes at −80 °C until analysis. Chl *a* was extracted from the filters and quantified following the methods listed in Golnick et al. (2016). In the laboratory, water samples warmed to room temperature were analyzed with a FluoroProbe (BBE Moldaenke) equipped with a bench-top cuvette reader, as previously described (Chaffin et al., 2013). The YSI EXO2 was used to record spot location Chl *a* and phycocyanin RFU data adjacent to the grab sample (approximately 0.25 m depth).

2.4.2. Cyanotoxins

Total MCs (lake water subject to three freeze-thaw cycles) and extracellular MCs (prefiltered with GMF, 0.45 μm pore) were quantified following the Ohio EPA protocol (Ohio EPA, 2021) with Gold Standard Diagnostics enzyme-linked immunosorbent assay (ELISA) kits (#520011; Warminster, PA, USA) on an Eurofins Abraxis automated Cyanotoxin Automated Assay System (CAAS Cube) instrument (#475006). All total MCs samples exceeded the working ELISA range of 5 μg L^{-1} and therefore were diluted 10x to 20x with deionized water. Extracellular MCs were quantified in the field-filtered samples with ELISA.

For a subset of samples (n = 12) from the mesocosm experiment, variants of microcystins, cylindrospermopsin, anatoxin-a, and anabaenopeptins were evaluated following the United States Environmental Protection Agency (US EPA) Method 544 sample collection and handling protocols (Shoemaker et al., 2015) for liquid chromatography-high resolution mass spectrometry (LC–HRMS) was performed on a Thermo QExactive Orbitrap, equipped with electrospray ionization (ESI) source. Both online-SPE loading and analytical separation utilized a Thermo Vanquish LC system equipped with a Vanquish C Quaternary Loading Pump and a Vanquish H Binary Elution Pump. A TriPlus RSH Autosampler (Thermo, USA) was used for sample handling. Targeted microcystin analyses included microcystin variants not included in Method 544 but which had commercially available standards. Cylindrospermopsins, anatoxin-a, and anabaenopeptins with commercially available standards were analyzed with microcystins on the same combined analytical run. Non-targeted analysis was performed to identify both microcystin variants not included in targeted analysis and possible transformation by-products. MS/MS fragmentation patterns were monitored to identify the typical ADDA fragment m/z = 135.08.

2.4.3. Dissolved organic carbon concentration and chemistry

Samples for dissolved organic matter analysis were stored at 4 °C until analysis, which occurred within 7 days of sample collection. DOC concentration was measured as non-purgeable organic carbon on a Shimadzu TOC-L Analyzer. UV–Vis absorbance was measured on a Horiba Jobin Yvon Aqualog. Then, the specific UV absorbance at 254 nm ($SUVA_{254}$) was calculated by dividing the absorbance at 254 nm by the DOC concentration (in mg L^{-1}) (Weishaar et al., 2003). $SUVA_{254}$ has units of L*mg C^{-1}*m^{-1} and increases linearly with the percentage of aromaticity of water samples (Weishaar et al., 2003). Oxidation of DOM by ozone will result in a lower bulk aromaticity, and thus lower $SUVA_{254}$.

2.4.4. Nutrients

Total phosphorus (P) and nitrogen (N) were measured on unfiltered samples following an alkaline persulfate digestion and quantified as phosphate and nitrate, as in Patton and Kryskalla (2003). Nitrate, nitrite, ammonium, and dissolved reactive P were quantified on the filtered water (same samples as the extracellular MCs) following standard methods, as listed in Chaffin et al. (2019). All nutrient analyses were conducted on a SEAL Analytical QuAAtro segmented flow auto-analyzer.

2.4.5. Cell viability by fluorescence microscopy

Samples from the mesocosm were stained with SYTOX™ Green (Invitrogen) to determine cell viability. SYTOX™ Green cannot cross intact cell membranes, but it will easily penetrate compromised membranes of dead cells and binds with nucleic acids (Hazlett et al., 2007). SYTOX™ Green results in dead cells fluorescing bright green, peak at 523 nm, and alive cells do not fluoresce. The samples were treated with 1 μmol L^{-1} SYTOX™ green stain, incubated in the dark for 5 min, and then viewed at 400x magnification with a M837FLR Series Trinocular Epi-Fluorescence Microscope with 18 MP USB 3.0 Digital Camera.

2.4.6. Aqueous ozone

First, the molar absorptivity of indigo (ε_{ind}) was determined as described by Gordon and Bubnis (2002). Ozone absorbance at 258 nm was measured using a Shimadzu UV-2401PC spectrophotometer. The absorbance of indigo solutions at 600 nm was measured using a Genesys 20 spectrophotometer (Thermo Scientific, Waltham, Massachusetts, USA). Both measurements used a 1-cm quartz cell and a reference cell containing deionized water. Ozone demand was determined as described by Richard (1994). Total ozone was measured using a modified indigo method (Kuhn, 2024). Indigo Stock Solution (ISS) was prepared according to Bader and Hoigné (1981). Indigo Reagent RIII and RIV were prepared according to Kuhn (2024).

Ozonated samples were prepared by adding 90 mL of NBOT effluent solution collected directly from the effluent nozzle to a 100-mL volumetric flask containing 10 mL RIII or RIV. The indigo method relies on a change in absorbance due to bleaching of indigo by ozone. Therefore, blank samples were collected outside of the enclosed location and prepared by adding 90 mL of untreated lake water to a 100-mL volumetric flask containing 10 mL RIII or RIV to account for matrix effects on indigo decolorization. Samples were filtered using a 0.45-μm polytetrafluoroethylene (PTFE) syringe filter prior to measuring absorbance. All samples were covered with aluminum foil and stored in the dark to prevent photodegradation of indigo.

The absorbances (600 nm) of each blank and ozonated sample were measured within 2 min of indigo addition. Replicate measurements of each ozonated and blank sample were taken for up to 10 days following the initial sampling date until indigo decolorization was negligible. Separately, ambient bromide and manganese concentrations in lake water were measured to confirm concentrations would not interfere with the indigo method. Total ozone measured was determined as described by Bader and Hoigné (1981).

2.5. Bacteria community analyses

2.5.1. DNA extraction, 16S rRNA and 18S rRNA Amplification and sequencing

Water samples were collected in sterile 1-L Nalgene bottles and stored on ice and at 4 °C before processing within 24 h of collection. Samples were filtered on 0.22-μm mixed cellulose filters (MilliporeSigma, Burlington, MA, USA) and stored at −80 °C. Samples collected near the east NBOT were chosen for sequencing. The sites

selected were: N (NBOT inlet), T (NBOT outlet), A (3 m from outlet) and site E (main lake control). DNA was extracted using the QIAGEN (Qiagen, Hilden, Germany) DNeasy Blood & Tissue kit with modified protocols established by (Djurhuus et al., 2017). The V4-V5 hypervariable regions of the 16S rRNA were amplified using 515FY-926R primer pair described in Parada et al. (2016). The 16S rRNA amplicon libraries were prepared and sequenced using paired-end (2 × 250 bp) Illumina NovaSeq (Novogene, Beijing, Peoples Republic of China).

2.5.2. Sequencing analysis

The 16S rRNA amplicon sequences were demultiplexed and assigned to specific sample IDs based on their multiplex identifier at Novogene using in-house bioinformatic pipelines. DADA2 (Callahan et al., 2016) was used to process raw sequences in R v4.0.0 (R Core Team). Briefly, paired-end reads were filtered, trimmed, and merged prior to dereplication and then analyzed for detection and removal of potential chimeras. Non-chimeric sequences were pooled together to define amplicon sequence variants (ASVs). Taxonomic assignment of ASVs was based on naïve Bayesian classifying method (Wang et al., 2007) using the 16S rRNA databases CyanoSeq (Lefler et al., 2023) for cyanobacteria and SILVA 138.1 (Quast et al., 2013) for bacteria. ASVs assigned to archaeal, chloroplast, eukaryotic, and mitochondrial taxa removed before being rarified to an even depth (Schloss, 2023), using the phyloseq package (McMurdie and Holmes, 2013). The vegan package (Oksanen et al., 2024) was used for statistical analyses, calculation of diversity indices, and generation of ordinations in combination with ggplot (Wickham, 2016) and MicroViz (Barnett et al., 2021). Alpha diversity was calculated using Shannon index; a Wilcoxon test was used to compare indices between each time point. The "adonis2" function of the vegan package was used to conduct a permutational multivariate analysis of variance (PERMANOVA) on robust Aitchison distances to test the effect of NBOT, date, and site on bacterial and cyanobacterial community composition.

2.6. Data analysis

The mesocosm data were analyzed by a repeated measure two-factor analysis of variance (RM-ANOVA) with time after NBOT treatment as the within-subject variables and NBOT treatment as the between-subject factor. The Greenhouse-Geisser statistic was interpreted for the within-subject effects (time after treatment and the interaction). Statistical analyses were conducted with IBM SPSS version 29. Contour plots for the SBE grab samples data for concentrations of chl *a*, total MCs, and $SUVA_{254}$ were made in Sigma Plot version 15 to display changes throughout the trial and distance of sample from the NBOT units. To determine the zone of influence of NBOTs, a subset of data from sites inlets, outlets, and 3.3 m were used and the percent relative difference (%RD) was calculated between the inlet and outlet and 3.3-m samples as:

$$\%RD = (C_2 - C_1) / C_1 \ *100\%$$

Where C_2 is the concentration measured at the outlet or the 3.3-m sample and C_1 is the concentration measured at the inlet. The %RD were then plotted against the O_3:DOC ratio measured at the NBOT inlet.

3. Results

3.1. Mesocosm experiment

DOC concentration in the mesocosm tanks before NBOT ranged between 6.88 mg C L^{-1} and 7.91 mg C L^{-1} (average of 7.20 mg C L^{-1}). The low, medium, and high applied ozone doses were 4.8 ± 0.6, 7.1 ± 0.8, and 15 ± 1 mg O_3 L^{-1}, respectively. The specific ozone to DOC ratios (O_3:DOC) were 0.68 ± 0.05, 1.21 ± 0.08, and 2.04 ± 0.07 in the low, medium, and high NBOT doses.

Chl *a* concentrations in all 15 tanks were 200 ± 20 μg L^{-1} (mean of all 15 tanks ± 1 standard error) immediately before NBOT treatment (Fig. 2A). The within-subjects interaction between time after treatment and NBOT treatment was significant ($p < 0.001$), which indicates that how chl *a* concentration changed across the time points depended on NBOT treatment, and the between-subject effect of NBOT treatment was significant ($p < 0.001$), which indicates that chl *a* concentration differed among NBOT treatments. In the control tanks Chl *a* concentrations were stable and similar to initial concentrations during the first 72 h and then decreased at hour 96. Tukey test indicated that there was no significant difference of chl *a* concentrations between the control and oxygen-only nanobubble control throughout the experiment. The low NBOT had intermediate chl *a* concentrations, and the medium and high NBOT had the lowest chl *a* concentrations. The decrease of chl *a* concentrations occurred the fastest in the high NBOT treatment, but then the medium and high NBOT treatments had similar chl *a* concentrations 24 h after treatment. Chl *a* concentrations in all three NBOT treatments increased on the final day of the experiment by 2X to 3X from the concentrations measured on hour 72.

Cyanobacteria biomass (measured as phycocyanin relative fluorescence units, PC-RFU) was 16.6 ± 0.1 immediately before NBOT treatment (Fig. 2B). PC-RFU followed a similar decline as chl *a* concentrations in response to the NBOT treatments, but PC-RFU did not rebound like chl *a*, indicating the chl *a* response was not due to cyanobacteria rebound. The within-subjects interaction between time after treatment and NBOT treatment was significant ($p < 0.001$) and the between-subject effect of NBOT treatment was significant ($p < 0.001$). The medium and high NBOT treatments both decreased PC-RFU to less than 0.1 units by hour 24. Low NBOT treatment decreased PC-RFU to 2.6 units. The oxygen-only control resulted in PC-RFU intermediate to the low NBOT and control.

Total MCs concentrations were 23 ± 2 μg L^{-1} and the extracellular MCs were 0.8 ± 0.1 μg L^{-1} (4.1% of MCs were extracellular) prior to NBOT treatment (Fig. 2C and D). The within-subjects interaction between time after treatment and NBOT treatment was significant ($p < 0.001$) but the between-subject effect of NBOT treatment was not significant ($p = 0.470$). Total MCs in the control increased throughout the experiment and peaked at 40 ± 10 μg L^{-1} at hour 72, while the extracellular fraction accounted for less than 6% of total MCs throughout the experiment. Total MCs in the oxygen-only control was stable and similar to initial concentrations throughout the experiment but had a slightly higher fraction of extracellular MCs than the control (up to 15 ± 7 % of total). Total MCs in all three NBOT treatments decreased throughout the experiment and the high NBOT treatment had the lowest total MCs among the NBOT treatments. Despite the lack of a between-subject effect significant difference, there were large differences among treatments at 96 h after treatment; total MCs were 3 ± 1 μg L^{-1}, 9 ± 3 μg L^{-1}, and 16 ± 9 μg L^{-1} in the high, medium, and low NBOT treatments, respectively. MCs were 100% in the extracellular phase after just 4 h in the high NBOT treatment and after 8 h in the medium NBOT treatment. MCs were also shifted to extracellular in the low NBOT treatment but peaked at only 80 ± 10% at hour 72.

The dominant MC variant present in all samples was [D-Asp3] MC-RR (89.6%–92.7% of total MCs), and [D-Asp3] MC-LR and [D-Asp3-(E)-Hhb7] MC-HphR were detected at lower concentrations (Supporting Information Table S1). Anabaenopeptin A and B were detected in all samples, with concentrations in initial (time 0) mesocosm samples from 2.01 μg L^{-1} for anabaenopeptin A and 4.17 μg L^{-1} for anabaenopetin B. Cylindrospermopsins and anatoxin-a were not detected. Total microcystins by targeted variant analyses were between 24 and 60% of totals determined by ELISA. This discrepancy may be explained by the presence of multiple unknown microcystins identified through non-targeted analyses, including potential isomers of [D-Asp3] MC-RR and [D-Asp3] MC-LR, and variable cross-reactivity of different variants in ELISA. In the mesocosm trial, anabaenopeptin A decreased by 65.0% and anabaenopeptin B decreased by 68.6% 24 h after treatment in the low and

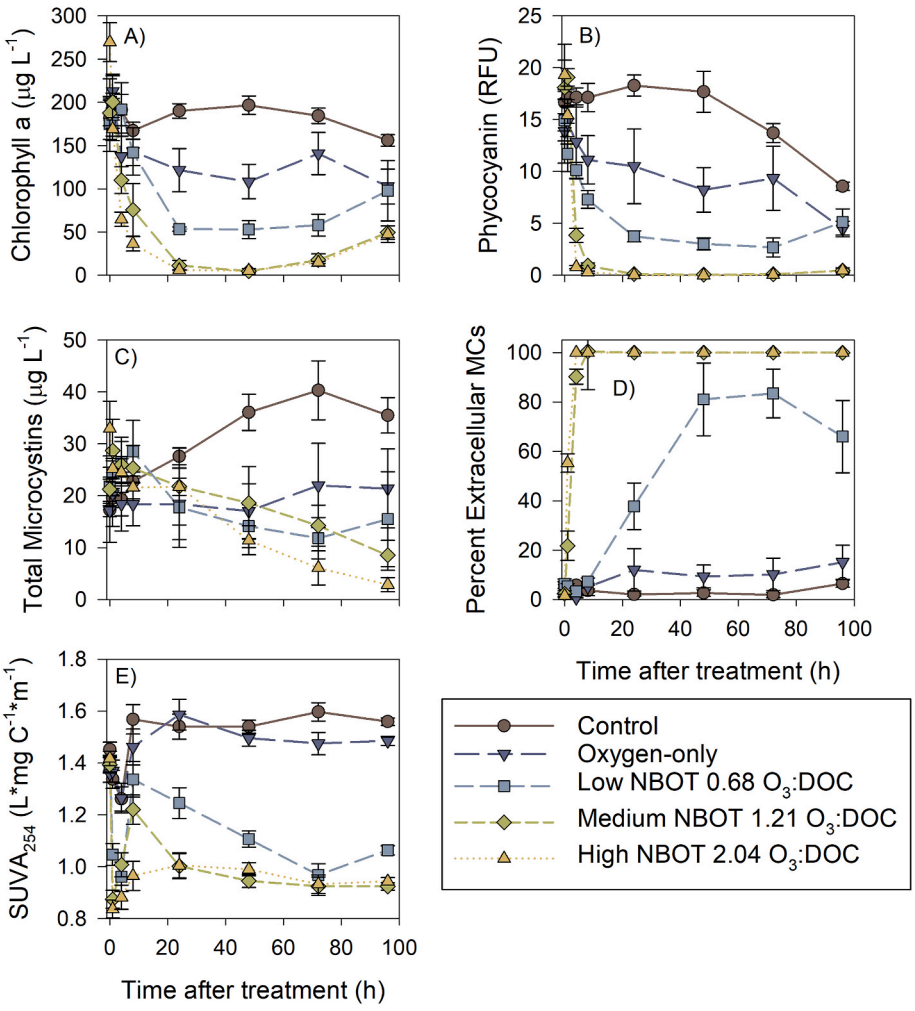

Fig. 2. The concentrations of A) chlorophyll (µg L^{-1}), B) phycocyanin (relative fluorescence units, RFU), C) total microcystins (µg L^{-1}), and D) the percentage of extracellular microcystins of total microcystins 96 h after NBOT treatment in the mesocosm experiment. Initial, hour 0, samples were collected prior to treatment.

medium NBOT dose treatments, respectively. The oxygen-only treatment only reduced anabaenopeptin A and anabaenopeptin B by 8.3% and 8.7%, respectively, after 24 h. The high NBOT dose treatment samples were lost in shipment and samples were not collected for LC-MS analyses at later time steps.

$SUVA_{254}$ was 1.41 ± 0.02 L*mg C^{-1}*m^{-1} in the initial samples (Fig. 2E). The within-subjects interaction between time after treatment and NBOT treatment and the between-subject effect of NBOT treatment were both significant ($p < 0.001$). $SUVA_{254}$ in the control and oxygen-only control increased to values ~1.5 by hour 24 and remained at 1.5 to 1.6 for the remainder of the experiment. $SUVA_{254}$ in the medium and high NBOT treatments decreased to ~0.9 by hour 24 and remained at 0.9 to 1.0 for the remainder of the experiment. $SUVA_{254}$ was slower to reach ~1.0 in the low NBOT (hour 72).

In the initial samples (Fig. 3A and C), *Planktothrix* filaments appeared red with SYTOX green stain fluorescence microscopy, indicating living cells. *Planktothrix* filaments in the control were red after 24 h of incubation (Fig. 3B), but there were a few small areas of green, likely from dead heterotrophic bacteria. All *Planktothrix* filaments were bright green in the high NBOT treatment, indicating dead cells (Fig. 3D). Many smaller heterotrophic bacteria were also dead.

3.1.1. *In-situ lake trial: ozone generation*

Gas phase ozone was measured on seven dates during 2023. The measured flow rate was 1.7 x 10^4 L h^{-1} per NBOT throughout the two 4-week in-situ trials. The ozone generated by the East NBOTs ranged from 58 g O_3 hr^{-1} to 158 g O_3 hr^{-1} (100 ± 10 g O_3 hr^{-1}), the West NBOTs ranged from 49 g O_3 hr^{-1} to 154 g O_3 hr^{-1} (110 ± 20 g O_3/hr). An ozone dose through the NBOT unit was determined using the average unit flowrate of 280 L min^{-1} (East: 3.4 mg O_3 L^{-1} to 9.3 mg O_3 L^{-1}, and West: 2.9 mg O_3 L^{-1} to 9.1 mg O_3 L^{-1}) (Table 1). Both NBOTs generated the lowest measured ozone on August 8, 2023, while the East NBOT generated the most ozone on June 14, 2023 and the West on July 5, 2024.

Readily degradable compounds react rapidly with and consume ozone before a residual is measured (Rakness, 2011). Ozone demand is the ozone dose added before any ozone residual is measured, corresponding to the amount of ozone consumed during these rapid reactions. The ozone demand at GLSM was determined with representative GLSM water to be 3.3 mg O_3 L^{-1} but will vary as DOC levels vary.

Aqueous ozone was measured on eight dates during 2023. The average initial aqueous ozone concentration in the outlet was 110 ± 110 µg L^{-1} reflecting variability in the ozone demand due to varying ozone gas phase concentrations and varying DOC. After the initial consumption of ozone due to the ozone demand, aqueous ozone concentration can be detected. Ozone diffusion from nanobubbles occurred and total ozone concentration was reached within 2 or 3 days after indigo addition. Average total ozone measured was 460 ± 270 µg L^{-1}. The difference between the initial and total concentration is bubble ozone, or ozone released from the diffusion of bubbles. The average bubble ozone was 65 ± 26% of the total ozone measured.

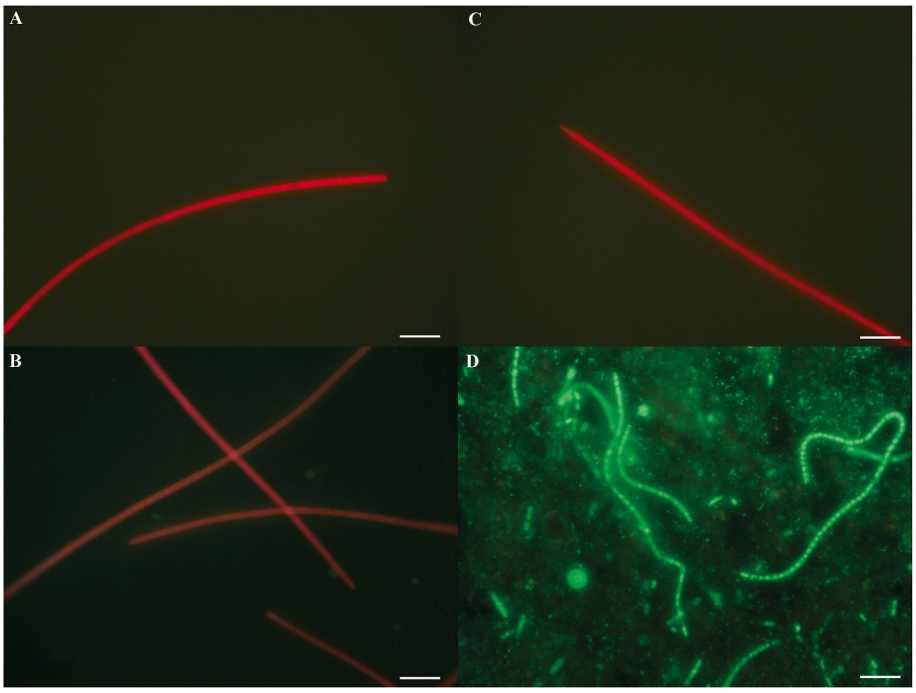

Fig. 3. Representative fluorescent micrographs of *Planktothrix* filaments stained with SYTOX green. Red indicates alive cells and green indicates dead cells. A) Control initial; B) Control after 24 h; C) NBOT high dose treatment prior to treatment; D) NBOT high dose 24 h after treatment. (For interpretation of the references to color in this figure legend, the reader is referred to the Web version of this article.)

Table 1
Ozone generated by the NBOTs used in the 2023 Sunset Beach enclosure (SBE) trial. A flow rate of 1.7 x 10^4 L/h was used to calculate mg L^{-1}. Dissolved organic carbon (DOC) are the average concentrations measured at all sites. The ozone to DOC dose were calculated by averaging the ozone dose from the two NBOTs. ND = no data.

	East NBOTs		West NBOTs		SBE average	
	Ozone		Ozone		DOC	
	g O_3/hr	mg O_3 L^{-1}	g O_3/hr	mg O_3 L^{-1}	mg C L^{-1}	O_3: DOC
14 June	157.63	9.28	111.10	6.54	12.90	0.61
20 June	ND	ND	ND	ND	13.13	ND
27 June	ND	ND	20.83	1.22	12.23	0.10
5 July	87.32	5.14	154.40	9.09	12.64	0.56
8 Aug.	57.60	3.39	49.16	2.89	9.13	0.34
16 Aug.	124.99	7.36	142.70	8.40	9.17	0.86
22 Aug.	87.32	5.14	154.40	9.09	9.12	0.78
29 Aug.	106.24	6.25	139.22	8.20	9.08	0.80

3.1.2. *In-situ lake trial: high temporal resolution data*

Water temperature of SBE was ~25 °C on May 31, 2023 when the data buoy was deployed (Fig. 4A). Water temperature decreased to 17.7 °C throughout the first half of June. Water temperature steadily increased from ~18 °C to 31 °C throughout the first NBOT treatment, ranged from 25.0 °C to 31.1 °C during the NBOT-off period, and was variable during the second NBOT treatment with declines and increases of several degrees. Diel patterns of temperature are visible.

pH was basic and ranged from 8.0 to 9.6 throughout 2023, and there was no association with NBOT treatments (Fig. 4B). Diel patterns in pH were observed with increased pH during the daytime and decreased pH at night.

Turbidity decreased from ~60 FNU to ~20 FNU during the first half of June (Fig. 4C). Turbidity steadily increased from ~20 FNU to ~70 FNU throughout June, July, August, and September and no association was observed with NBOT treatments. FNU measurements were highly variable over a short time window (<1 h) as FNU often deviated by up to 20 FNU.

Dissolved oxygen concentration corrected for temperature (percent saturation, DO%) showed wide diel fluctuations from 50% saturation at nighttime to over 300% during the daytime (Fig. 4D)

Phycocyanin relative fluorescence (PC RFU) decreased from ~17.5 to 10.5 RFU during the first week of NBOT treatment, but then increased to ~25.5 RFU during the second week of treatment, and then decreased to ~16 RFU by the end of the first treatment (Fig. 4E). PC RFU increased to ~23.5 RFU during the NBOT-off period. PC RFU was variable during the second NBOT treatment as PC RFU ranged from ~18.0 to 25.5 RFU. The highest PC RFU of ~29.1 were recorded in mid-September, one week after the second NBOT treatment ended.

Chlorophyll RFU was much lower than PC RFU and ranged between 2 and 3 RFU all of 2023 (Fig. 4F).

Fluorescence dissolved organic matter (fDOM) RFU increased from 10.8 to 21.5 RFU during the first half of the first NBOT treatment, and then fDOM decreased to ~13 RFU by the end of the first NBOT treatment (Fig. 4G). fDOM was stable and ranged between 12 and 13 RFU for the remainder of 2023 and no difference was recorded during the second NBOT treatment.

3.1.3. *In-situ lake trial: grab samples*

There was no apparent spatial or temporal association of filtered-extracted chl *a* concentrations and the NBOT deployments. Across all sites, filter-extracted chl *a* concentrations averaged 171 ± 10 μg L^{-1} (mean ± standard error) and 178 ± 6 μg L^{-1} on 3 May and 6 June, respectively, prior to NBOT deployment (Fig. 5). During the first two weeks of NBOT deployment, chl *a* concentrations decreased to 161 ± 3 μg L^{-1} and 139 ± 3 μg L^{-1} on 14 June and 20 June, respectively, but then increased to 220 ± 10 μg L^{-1} on 26 June during the third week of NBOT deployment. These temporal patterns were observed at all sites within the SBE treatment zone and at the control sites in the main lake (Fig. 5). During the NBOT-off period between 10 July and 6 August, chl *a* concentrations ranged from 174 ± 4 μg L^{-1} to 214 ± 5 μg L^{-1}. Chlorophyll *a* concentrations in August and September were greater than that observed during June and July, and this pattern was observed at all

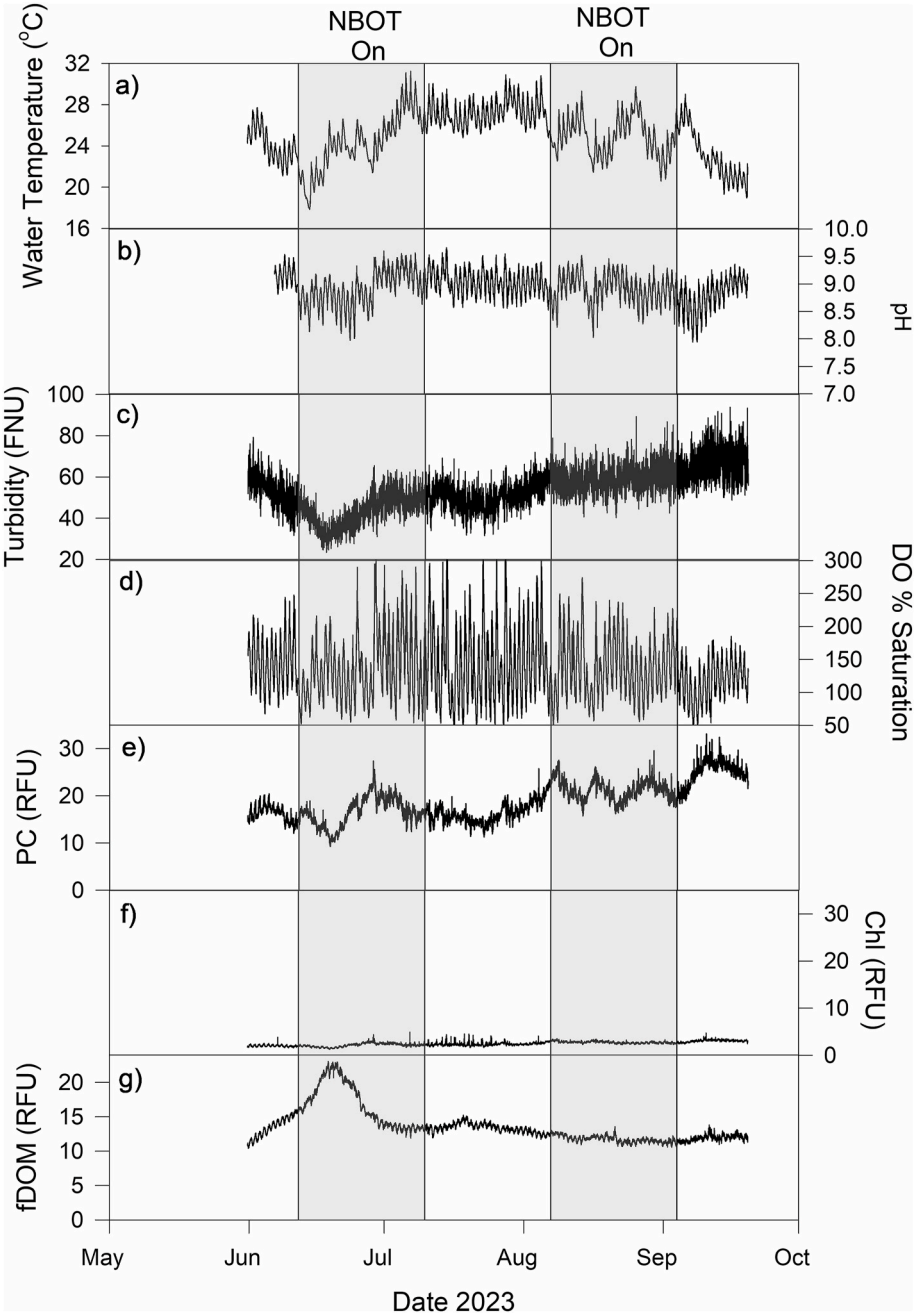

Fig. 4. High temporal resolution dataset recorded from a buoy deployed in the center of Sunset Beach enclosure (~100 m from the east NBOT and 130 m from the west NBOT). The shaded gray areas represent when the NBOT units were deployed.

sites. During the second 4-week NBOT deployment, chl *a* concentrations ranged from 264 ± 4 μg L^{-1} to 293 ± 4 μg L^{-1}. Following the NBOT deployment, chl *a* concentrations ranged from 253 ± 4 μg L^{-1} to 308 ± 7 μg L^{-1}.

YSI EXO2 PC-RFU and FluoroProbe cyanobacteria-chl *a* gave similar patterns as filter-extracted chl *a* concentration (Supporting Information Fig. S1), and these variables were strongly correlated with filter-extracted chl *a* (r = 0.869, 0.863, respectively; Supporting Information Table S2). The FluoroProbe did not detect any green algae nor diatoms in any SBE sample, and the ratio of PC-RFU to chl-RFU exceeded 1.0 in every sample and was greater than 5.0 in 89% of samples. Collectively, these data indicated that eukaryotic phytoplankton were very minor component of the SBE plankton community. Because the fluorescence sensors can have interferences due to the physiological state of plankton (Beardall et al., 2001; Chang et al., 2012), colonies vs. single cells (Hodges et al., 2017), the presence of extracellular PC (Bastien et al., 2011), which is likely following NBOT and algaecides (Tsai et al., 2024), we use the filter-extracted chl *a* concentration as the surrogate for cyanobacteria biomass in SBE throughout this report.

There was no apparent spatial or temporal association of total MC concentrations and the NBOT deployments. Total MC concentrations were 23 ± 4 μg L^{-1} and 24 ± 5 μg L^{-1} on 3 May and 6 June, respectively, prior to the first NBOT deployment (Fig. 6). Total MC concentrations increased during the first 4-week NBOT deployment with ranges from 34 ± 2 μg L^{-1} to 67 ± 3 μg L^{-1}. These temporal patterns were observed at all sites within the SBE treatment zone and at the control sites in the main lake (Fig. 6). Total MC concentrations decreased from 36 ± 3 μg L^{-1} on 12 July (2 days after NBOTs were turned off) to 20 ± 1 μg L^{-1} on 2 August. Total MCs increased again during the second NBOT deployment with ranges from 49 ± 2 μg L^{-1} to 58 ± 2 μg L^{-1}. The highest total

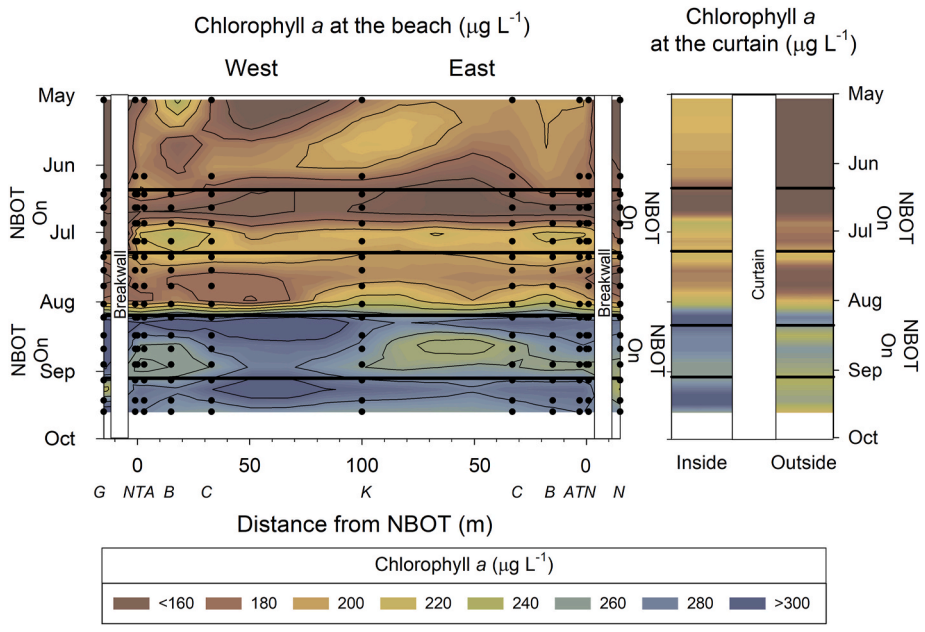

Fig. 5. Filter-extracted chlorophyll *a* concentration (μg L^{-1}) at the beach (left larger panel) and at the curtain (smaller right panel) of Sunset Beach enclosure during 2023. The X axis in the beach panel represents the distance from the west and east NBOT outlets, and the letters beneath the X axis are site names on Fig. 1. Sites G, N, and Outside were collected from the main lake outside of Sunset Beach enclosure. The horizontal lines represented when the NBOTs were turned on and off. Note that the color scale begins at 160 μg L^{-1}, not zero. The dots on the isopleth indicate when and where grab samples were collected. (For interpretation of the references to color in this figure legend, the reader is referred to the Web version of this article.)

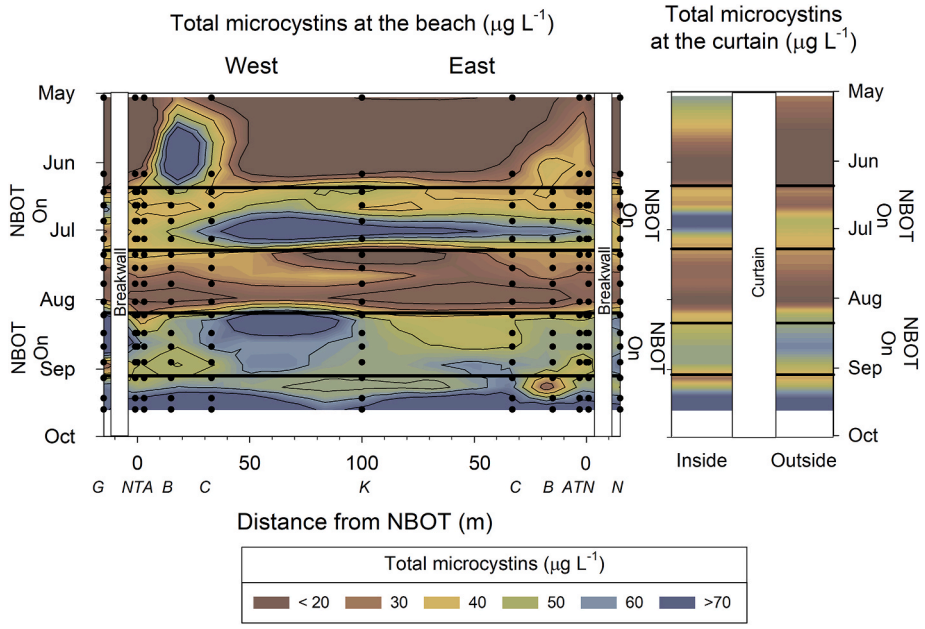

Fig. 6. Total microcystins (μg L^{-1}) at the beach (left larger panel) and at the curtain (smaller right panel) of Sunset Beach enclosure during 2023. The X axis in the beach panel represents the distance from the west and east NBOT outlets, and the letters beneath the X axis are site names on Fig. 1. Sites G, N, and Outside were collected from the main lake outside of Sunset Beach enclosure. The horizontal lines represented when the NBOTs were turned on and off. Note that the color scale begins at 20 μg L^{-1}, not zero. The dots on the isopleth indicate when and where grab samples were collected. (For interpretation of the references to color in this figure legend, the reader is referred to the Web version of this article.)

MCs concentrations, 83 ± 3 μg L^{-1}, were measured on the last sample date of 19 September when the NBOTs were off. The majority of MCs were intracellular as extracellular MCs accounted for less than 10% of total MCs following the NBOT deployments (Supporting Information Fig. S1).

Dissolved organic carbon decreased from 16 ± 2 mg C L^{-1} measured on 6 June to concentrations that ranged between 9.1 ± 0.05 to 10.2 ± 0.03 mg C L^{-1} during August and September (Supporting Information Fig. S4). The lowest average $SUVA_{254}$ was measured on 20 June at 1.14 ± 0.01 L* mg C^{-1}*m^{-1} and was greater than 1.26 ± 0.07 L*mg C^{-1}*m^{-1} for the rest of June (Supporting Information Fig. S5). $SUVA_{254}$ increased throughout July and August (peaked at 1.80 ± 0.02 on 8 August) and decreased during September (Supporting Information Fig. S5). There was no apparent spatial or temporal association of $SUVA_{254}$ and the

NBOT deployments.

The weekly averages of total P, DRP, and total N ranged from 271.5 to 430.6 μg P L^{-1}, 18.4–90.6 μg P L^{-1}, and 3091.8 to 4704.1 μg N L^{-1}, respectively (Supporting Information Figs. S6, S7, S8), indicating a hypereutrophic environment. There was no association with the timing of NBOT treatments. The majority of the total N was in the organic fraction because concentrations of nitrate and nitrite were frequently less than the method detection limit of 10 μg N L^{-1}, and ammonium/ammonia was frequently less than 20 μg N L^{-1}.

3.1.4. *In situ lake trial: zone of influence*

Analysis of all SBE data indicated there was no association with the variables we measured and the timing of NBOT deployments. Therefore, we analyzed a subset of sites (NBOT inlet, outlet, and 3.3-m from the NBOT outlet) and the 8 weeks of data when the NBOTs were deployed to determine if there was a finer spatial scale of NBOT influence. Chlorophyll *a* concentrations at the outlet and 3.3 m from the outlet were within ±10% relative difference (%RD), but one outlet sample that had a relatively high O_3:DOC (0.93) had a chl *a* %RD of −34.3% (Fig. 7A). Total MCs showed a similar pattern as chl *a* and the sample with O_3:DOC of 0.93 had the largest negative %RD of −94.9% (Fig. 7B). However, two other samples had higher O_3:DOC (0.96, 1.03) and their %RD for chl *a* and MCs were less than ±10% and ±20%, respectively. For extracellular MCs, three outlet samples had higher %RD than the inlet, but one these samples was observed at the lowest O_3:DOC (Fig. 7C). The outlet sample highlighted for chl *a* and total MCs with O_3:DOC of 0.93 had a very high %RD for extracellular MCs. $SUVA_{254}$ had a clearer pattern of outlet samples having a lower %RD than the 3.3 m sample, and this pattern was observed across the entire range of O_3:DOC (Fig. 7D).

3.1.5. *In situ lake trial: community composition*

A total of 1,789,040 high-quality reads were generated after low-quality reads were filtered, a total of 5061 unique ASVs were recovered after removal of non-target taxa, 339 of the total ASVs were cyanobacterial. As expected, the most abundant cyanobacterial genus was *Planktothrix*, which frequently comprised >90% of the cyanobacterial relative abundance (Fig. 8A). Other bloom-forming genera were present (e.g., *Aphanizomenon*, *Dolichospermum*, *Raphidiopsis*, etc.) although their abundances were lower and only began to increase in August and September. Overall, cyanobacterial communities showed no significant differences between NBOT on or off (PERMANOVA: $R^2 = 0.02$, $F = 1.06$, $p = 0.29$) nor between sampling site (PERMANOVA: $R^2 = 0.06$, $F = 0.92$, $p = 0.56$). There was no significant difference in alpha diversity of cyanobacteria when the NBOT was on or off (Fig. 8B), nor between sampling location (Fig. 8C) (ANOVA: $p > 0.05$). There were significant differences between cyanobacterial communities based on date (Fig. 8D) (PERMANOVA: $R^2 = 0.18$, $F = 7.6$, $p < 0.0001$) increasing through the course of the treatment.

Likewise, the total bacterial communities were similar when NBOT was turned on or off (Supporting Information Fig. S9A). Class Cyanophyceae, was the most dominant bacterial class, followed by Actinobacteria and Gammaproteobacteria. There were no significant differences between communities when NBOT was on or off (PERMANOVA: $R^2 = 0.03$, $F = 1.41$, $p = 0.10$) nor site (PERMANOVA: $R^2 = 0.05$, $F = 0.84$, $p = 0.74$). There were no significant difference in alpha diversity of bacterial communities when the NBOT was on or off, nor

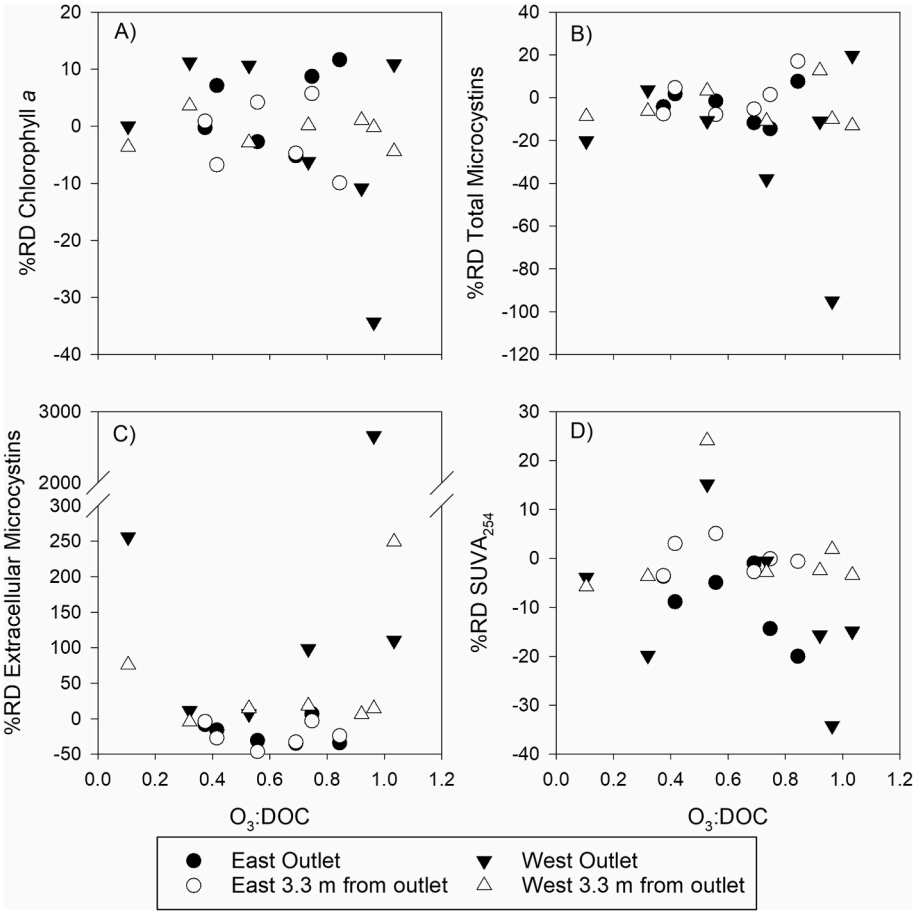

Fig. 7. The NBOT zone of influence for chlorophyll, total microcystins (MCs), extracellular MCs as the percentage of total MCs, and $SUVA_{254}$. The percent relative difference between the inlet and outlet (filled symbols) and 3.3 m from the outlet (open symbols) as a function of the ozone generated (mg O_3 L^{-1}) to dissolved organic carbon measured (mg C L^{-1}) in the inlet (O_3:DOC). The east NBOT are the circles and west NBOT the triangles.

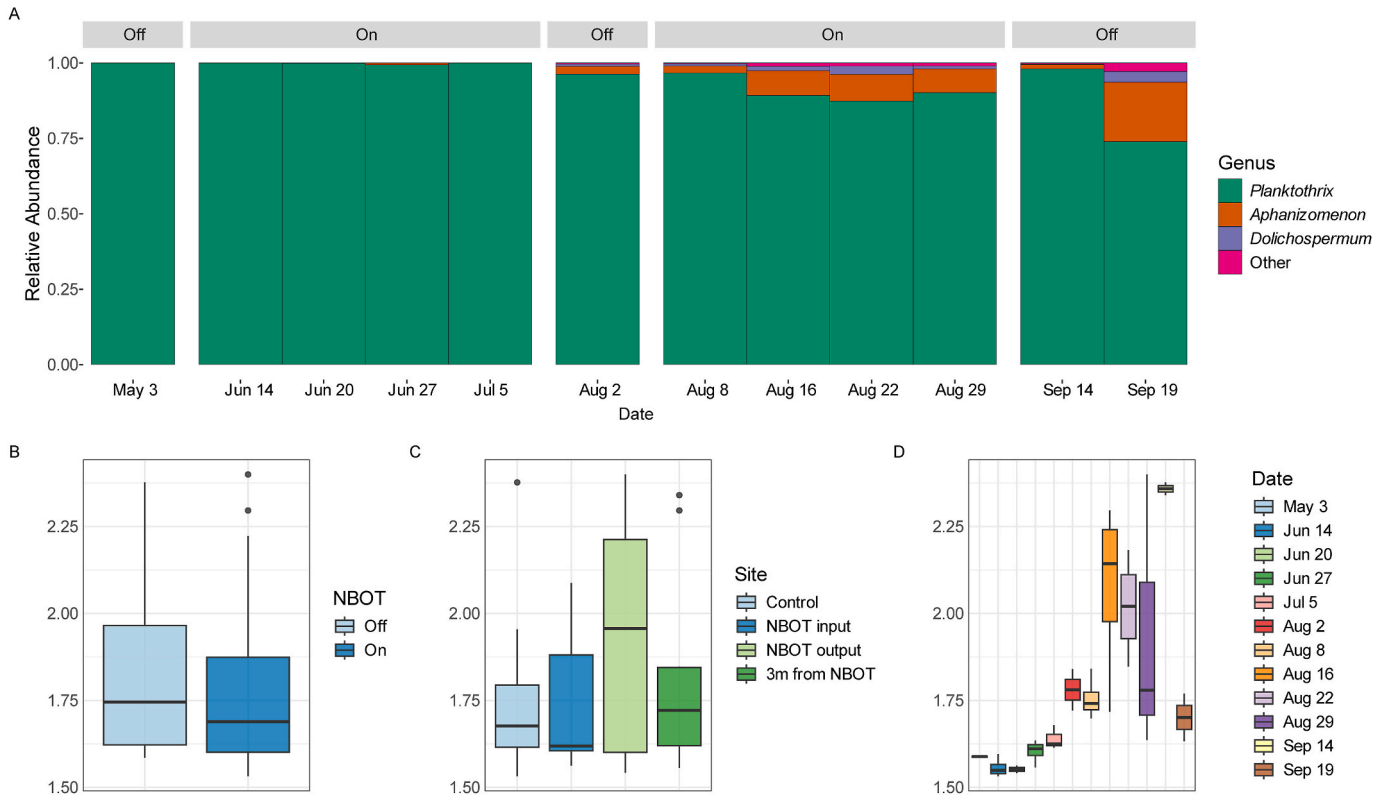

Fig. 8. The cyanobacteria community composition of the Sunset Beach Enclosure during 2023. In the top Row, panel A, "off" and "on" indicates when NBOTs were operating. Panel B: Shannon diversity of cyanobacterial communities when NBOT was on vs off C: Shannon diversity between different sample sites, D: Shannon diversity of each sampling date.

between sampling locations (Supporting Information Fig. S9B, C) (ANOVA: $p > 0.05$) There was a significant difference based on date (PERMANOVA: $R^2 = 0.22$, $F = 10.2$, $p < 0.0001$) and alpha diversity increased throughout the course of the treatment (Supporting Information Fig. S9D).

4. Discussion

4.1. NBOT efficacy for cyanoHAB control

GLSM is one of the most hypereutrophic lakes in North America with near year-round high-biomass (chl *a* > 100 μg L^{-1}) and high MC concentration (>20 μg L^{-1}) cyanoHABs (Jacquemin et al., 2023b; Mishra et al., 2019), and lake managers are searching for viable cyanoHAB control options. NBOT was effective at treating the high-biomass *Planktothrix*-dominant cyanoHAB sourced from GLSM in the 2200-L mesocosm trials, with clear indicators of 98–99% reductions in chl-*a* and phycocyanin and reduced microcystins and anabaenopetin concentrations. NBOT was ineffective at treating the *Planktothrix*-dominant cyanoHAB at the 4.76 x 10^7-L SBE field scale. The mesocosm cyanoHAB, however, was diluted with 60% filtered Lake Erie water and resulted in a lower DOC concentration and biomass and reduced oxidant demand than in the SBE field trial. The failure of the limited duration NBOT trial in SBE does not mean the technology does not hold promise in other lakes with less severe cyanoHABs, lower DOC, or smaller volumes. Additionally, it is recommended by the US EPA and others to treat a lake when harmful cyanobacteria cell counts are low (<10,000 cells mL^{-1}) or before the bloom fully develops (US EPA, 2015; Ohio EPA, 2020; Sukenik and Kaplan, 2021). The NBOT lake trial was initiated after cyanobacteria biomass had already reached a high concentration (>100 chl *a* μg L^{-1}) and elevated pH (pH > 9). In a prior study conducted in 2011 and 2012, chl *a* concentrations in GLSM in June ranged from 93 to 283 μg L^{-1} with corresponding *Planktothrix agardhii* cell counts of 3.25–5.40 x 10^6 cells mL^{-1}, concentrations well above recommended treatment levels (Dumouchelle and Stelzer, 2014). Thus, NBOT treatment efficacy in GLSM may have been increased if treatment was initiated earlier when biomass was lower (as is typically recommended) and/or if additional treatment units were utilized to try to increase both volume treated and O_3:DOC. It remains to be determined at what lake volume and/or O_3:DOC NBOT should not be considered a viable cyanoHAB treatment option, as both factors appear to be important predictors of success.

There are differences in how NBOT and traditional chemical-based algaecides are typically applied to a lake. These differences must be recognized when interpreting our data from the mesocosm and SBE trial. In this discussion, we use the term "lake" in reference to either an area of the lake to be treated (i.e., SBE in our study) or the entire body of water. First, NBOT treatments in our in-situ trial were confined to the lake shoreline relying on diffusion and advection of the ozone nanobubbles to reach other areas of the lake. Secondly, NBOT typical mode of operation is to run continuously, similarly to traditional aeration systems. For example, in our SBE in-situ trial, NBOTs operated continuously for two 4-week periods. On the other hand, algaecides are typically spread across the entire lake surface (or a more targeted area) by boat or from a sprayer on shore within a short period of time (hours to days) but with repeated periodic applications (Matthijs et al., 2012). While fixed location NBOT units were utilized in the SBE trial, there have been a few cases where boat mounted NBOT units were used to more quickly cover a larger surface area, however, that delivery mechanism was not evaluated here. Similarly, water systems sometimes continuously dose algaecides from a point location (near an intake, for example), instead of attempting to treat the entire lake surface.

The application of ozone in water and wastewater treatment has been used for decades. Because organic matter is present in much larger

concentration than constituents such as micropollutants and microorganisms, specific ozone dose, the concentration of ozone (mg L^{-1}) to DOC (mg C L^{-1}) is an important design parameter (Czekalski et al., 2016; Lee et al., 2013; Wolf et al., 2019). Therefore, the O_3:DOC dose is also an important consideration in cyanoHAB and cyanotoxin control by NBOT. For example, the oxidation of 500 μg L^{-1} microcystin-LR (MC-LR) in pure water (DOC 0.3 mg C L^{-1}) by an ozone concentration of 0.2 mg O_3 L^{-1} resulted in complete degradation of the MC-LR within 2 min (Shawwa and Smith, 2001); but, when DOC concentration was increased to 5 mg C L^{-1}, MC-LR degradation by 0.2 mg O_3 L^{-1} dropped by 90% (Shawwa and Smith, 2001). In these two examples, the ozone-to-DOC ratio (O_3:DOC) was 0.66 and 0.04, respectively.

Furthermore, there are two different scales of O_3:DOC to consider: 1) O_3:DOC ratio of cyanoHAB water flowing through the NBOT unit as ozone is injected into the water, and 2) the ozone mass dose to the total mass of DOC in the receiving body of water. The O_3:DOC ratio is affected by several factors. On the inlet and outlet scale, O_3:DOC is only affected by the amount of ozone generated and the DOC concentration in the influent water. On the lake scale, the total ozone generated is a function of the number of NBOT units, how much ozone each NBOT generates, and how long the NBOT units are operating. The total mass of DOC in the lake is a function of the DOC concentration and the lake volume. Hence, as lake volume increases and/or as biomass or DOC increases, the O_3:DOC ratio will decrease, and the effectiveness of NBOT will decrease unless there is a corresponding increase in the number of NBOT units. In our SBE in-situ trial, the average combined ozone generated per hour by the two NBOT units was 210 g h^{-1} and the combined flow rate 3.4 x 10^4 L h^{-1}, which gives an ozone dose 6.1 mg O_3 L^{-1} on a volume basis, and this dose per volume was in between the low (4.8 mg O_3 L^{-1}) and medium (7.1 mg O_3 L^{-1}) dose treatments of the mesocosm experiment. The average DOC concentration in SBE was 11.2 ± 0.1 mg C L^{-1}, and therefore the O_3:DOC ratio at the NBOT's inlet and outlet were 0.54. Due to the higher DOC concentration in SBE than the mesocosm, the average O_3:DOC ratio at the SBE NBOT units was less than the low NBOT dose of the mesocosm. However, this ozone dose (6.1 mg O_3 L^{-1}) and per DOC (0.54) at the NBOT inlet/outlet in SBE was also rapidly diluted by the rest of SBE.

To calculate the total ozone load to SBE, the average ozone per hour (210 g h^{-1}) resulted in 5.1 kg d^{-1}. Based on the average DOC concentration (11.2 ± 0.1 mg C L^{-1}) and the volume of SBE (4.76 x 10^7 L), 531 kg DOC was present in SBE. Therefore, the ratio of the cumulative ozone load SBE to the total mass of DOC in SBE was 0.0097, which is two orders of magnitude lower than the O_3:DOC of the low NBOT treatment (0.68) in the mesocosm study. Throughout a 28-day NBOT trial, a total of 143 kg of ozone were generated, and assuming a stable DOC concentration, the O_3:DOC ratio would be 0.27, less than half both the low NBOT dose in the mesocosm experiment (O_3:DOC 0.68) and the dose Shawwa and Smith (2001) observed complete MC-LR degradation at O_3:DOC of 0.66. This helps explain why a decrease in chl *a* and MCs in SBE was not observed.

The data from the mesocosm experiment clearly indicate that NBOT has the ability to kill *Planktothrix* cells from a high biomass bloom, decrease chl *a* concentrations, and oxidize DOC (decrease $SUVA_{254}$) within hours and days after treatment. Additionally, total MCs concentrations decreased by 62% and 92% of initial concentrations by hour 96 in the medium and high NBOT treatments, respectively, although MCs were released from the cells within 4–8 h of NBOT treatment. The degradation of MCs in the experiments may be attributed to ozone because the higher ozone dose decreased MCs (Shawwa and Smith, 2001). Ozone has also been shown to enhance biological degradation of contaminants (Peterson and Summers, 2021). Furthermore, the decrease in $SUVA_{254}$ in the NBOT outlet compared to inlet from the SBE trial confirms ozone reaction with organic matter passing through the unit. However, besides $SUVA_{254}$ from the outlet, there was no evidence that NBOT affected the cyanoHAB in SBE. In the mesocosm setting, the DOC concentrations were lower and all of the treated water was contained in a small volume where the ozone continued to react for 96 h. Whereas in SBE, the treated water was very quickly mixed with untreated water and the high pH in SBE increased ozone decay (i.e., decreased the O_3:DOC), and no effect was observed further than 3 m from the outlet. For example, in SBE the two NBOT units only treated 1.71% of the SBE volume in a 24-h period. While it may not be necessary to treat the entire volume in 24 h, it remains unknown what percentage of a lake should pass through NBOT units to be effective at decreasing bloom biomass under varying DOC and lake volume conditions. Additional controlled mesocosm experiments and field trials under varying DOC and percent water treated scenarios are needed to develop NBOT operational guidance for cyanoHAB control.

For waters used as a drinking water source, NBOT operational guidance would also have to consider potential for release of extracellular cyanotoxins and plan to subsequently degrade the extracellular cyanotoxins. Lab experiments have demonstrated the efficacy of ozone for microcystins oxidation at varying O_3:DOC and many drinking water plants rely on ozone as an effective treatment barrier for microcystins (via both direct oxidation and enhanced biological filtration). The City of Celina, Ohio, which utilizes GLSM as a source water and has some of the highest inlet microcystins concentrations (>100 μg L^{-1}) in the United States (Newell et al., 2024), relies on two-stage ozone treatment as an extracellular microcystins treatment barrier. In Celina's drinking water treatment facility ozone is dosed after dissolved air flotation (first stage) and again after sand filtration (second stage) prior to granulated activated carbon treatment (GAC), with ozone enhancing the biological filtration through the GAC. Since water has already been pre-treated prior to ozonation, the O_3:DOC is increased. The mesocosm experiments demonstrated the potential for NBOT for both cyanoHAB treatment and subsequent degradation of extracellular microcystins in source waters. The O_3:DOC ratio and percent source water treated would be critical for understanding if treatment was adequate for toxin destruction. Algaecide treatments pose a similar risk of release of extracellular toxins and that is why many states and countries place use restriction on algaecide applications to cyanoHABs within drinking water sources, including limiting applications to early-stage low biomass and/or lower cyanotoxin concentration blooms. Similar guidance might be prudent for NBOT treatment within drinking water sources. Unlike algaecides, however, NBOT has a greater potential to reduce extracellular toxins as part of combined treatment and may be a superior treatment option within drinking water sources. Furthermore, NBOT should only be an option for lakes that have bromine concentrations less than 50 μg L^{-1} to avoid bromate formation, especially at high pH associated with cyanoHABs (Morrison et al., 2023). The City of Celina's drinking water treatment plant has utilized ozone as a primary treatment barrier for MCs destruction for over a decade. The plant was required to test GLSM for bromide prior to receiving plan approval for an ozone system and samples drinking water for bromate monthly. Bromide was not detected in GLSM above the reporting limit and bromate was not detected in the drinking water above the reporting limit in 2022 and 2023 (City of Celina, 2022; City of Celina, 2023; Ohio EPA, 2024).

Copper and hydrogen peroxide-based algaecides are commonly used to control cyanoHABs and the concentrations of copper and hydrogen peroxide applied range between 0.3 and 1.0 mg Cu L^{-1} and 2–22 mg H_2O_2 L^{-1} (Kinley-Baird et al., 2021; Lefler et al., 2022). Given the volume of SBE, a one-time copper algaecide application would range from 14.3 kg to 47.6 kg, and a hydrogen peroxide application would range from 95.1 kg to 1046 kg. However, note that multiple one-time doses of algaecides may be required to control cyanoHABs and historic algaecide treatments have been ineffective at cyanoHAB control in SBE (Section 4.2). Use of algaecides is also becoming restricted, due to potential impacts on non-targeted organisms (Burford et al., 2019). The 28-d cumulative ozone load to SBE was 144 kg and is within the active ingredient application of the traditional algaecides. However, a single algaecide application can occur within hours, whereas the NBOT application was spread out over 28 days. The low percentage of lake

volume treated (1.7% d^{-1} over 28 days) and lower O_3:DOC factors into the lack of effect NBOTs had on cyanoHABs in SBE during 2023.

4.2. History of GLSM treatments

GLSM has a long history of failed or low efficacy in lake treatments spanning from simple compressed air aeration to algaecides to P binding chemicals, demonstrating the difficulty in treating the perennial high biomass *Planktothrix*-dominated GLSM bloom. Among the most widespread of these treatments include attempts to reduce available P through application of aluminum sulfate (alum). There is a history of six small scale pilot projects (2010–2011) attempted in localized embayments (e.g. Harmon's Channel, Otterbein Channel, West Bank Marina, Kozy Marina, Windy Point Marina, State Park Bay) as well as larger partial lake treatments (2011–2012), such as the one conducted by the State of Ohio which dosed between 30 and 40% of the lake area (Nogaro et al., 2013). More recently, an alum application was conducted in the SBE during 2020 which, similar to others in the past, saw immediate declines in algal biomass (up to 65% decreases in chlorophyll), however these numbers began to rebound within a week, reaching pre application levels within a few weeks (Davidson et al., in press). At the same location in 2021 the SBE received multiple doses of a copper-based algaecide followed by a lanthanum-based clay P binding treatment (Phoslock), exhibiting similar levels of immediate effect with a gradual leveling off and ramping up days later (in most cases) reaching non detectable efficacy levels within a few weeks (Davidson et al., in press). There are many examples where algaecides and alum treatments are successful at controlling cyanoHABs (ITRC, 2020; Osgood et al., 2017), and it is unclear what conditions led to the failure of these traditional control strategies in GLSM. The high *Planktothrix* abundance, year-round multi-year persistence of the bloom, elevated nutrients, and shallow water depths may all be contributing factors. Despite this long history of trial and error it should be mentioned that water quality in the watershed has improved tremendously over the past decade as a result of a combination of voluntary and obligatory conservation practices (Jacquemin et al., 2018). Perhaps most significantly, there have been strides towards restoring natural wetland habitat across the watershed with many of these sites demonstrating impressive improvements to water quality entering GLSM (Jacquemin et al., 2023a).

4.3. Oxygen-only nanobubble treatment

The mesocosm trials demonstrated that oxygen-only nanobubble treatment was ineffective for cyanoHAB control. Unlike the NBOT treatments, there was no significant difference in chl-a concentration between oxygen-only nanobubble treatments and controls and there was only a slight reduction in PC-RFU, with high variability between oxygen-only nanobubble treatment tanks. This is consistent with results from replicated small pond trials using oxygen-only nanobubble treatment (Laughinghouse IV et al., 2024). One of the purported modes of action from oxygen-only nanobubble treatment is production of hydroxyl radicals and hydrogen peroxide during nanobubble collapse; however, hydrogen peroxide concentrations did not differ from controls in the previously mentioned pond study (Laughinghouse IV et al., 2024). The slight differences in PC-RFU between controls and oxygen only nanobubble treatments in the mesocosm experiments (Fig. 2) could potentially be explained by mechanical shearing of cyanobacteria filaments within the NBOT unit and/or increased oxygen concentrations in the treatment tanks. These findings are important since there is limited peer reviewed literature on efficacy of oxygen-only nanobubble treatment, yet numerous companies are marketing the technology for cyanoHAB control. There is, however, some laboratory data on the potential for oxygen nanobubble treatment to enhance traditional alum and clay-based phosphorus treatments in sediments, but field data are limited and more research on potential for enhanced phosphorus control is needed (Waters et al., 2022).

5. Conclusion

The NBOT experiment in the mesocosm highlights the potential application of NBOT to control cyanoHABs, even at high initial biomass concentrations. However, the NBOT trial in SBE did not show an impact on cyanoHABs. Future applications of NBOT to control cyanoHABs should account for 1) DOC concentration, 2) phytoplankton biomass, and 3) the volume of cyanoHAB-affected water in the lake intended for treatment. Further research is needed to optimize the NBOT dosage based on O_3:DOC, determine the percentage of a lake that needs to pass through the NBOT unit(s), and determine the effectiveness and appropriate dosage for different cyanoHAB genera. Once an optimum dose is determined, one can estimate the energy costs needed to run NBOT (i.e. electrical energy per order). Furthermore, the potential cascading impacts of NBOT on lake ecology must be assessed because the change in DOC chemistry (i.e., $SUVA_{254}$) may affect the food resources for heterotrophic microbes. There is also a need to review the efficacy of existing cyanoHAB control strategies (i.e. algaecides and phosphorus binding agents) to help determine what lake conditions (DOC, volume, cyanoHAB biomass, water chemistry, temperature, light levels) and the right dose when they will be effective or ineffective and wasteful. Given the ineffectiveness of multiple, diverse, cyanoHAB control treatments in GLSM, there may be some conditions where lake managers should not waste resources attempting to control an existing high biomass bloom. In these instances, lake managers could focus on longer-term cyanoHAB prevention approaches, including nutrient reduction strategies, and consider treating future cyanoHABs earlier in a bloom season before DOC and biomass become elevated.

CRediT authorship contribution statement

Justin D. Chaffin: Writing – review & editing, Writing – original draft, Visualization, Supervision, Project administration, Methodology, Investigation, Funding acquisition, Formal analysis, Data curation, Conceptualization. **David E. Berthold:** Writing – review & editing, Validation, Methodology, Investigation, Data curation. **Eugene C. Braig:** Writing – review & editing, Project administration, Funding acquisition, Conceptualization. **Josh D. Fuchs:** Writing – review & editing, Methodology, Investigation, Data curation. **Rachel S. Gabor:** Writing – review & editing, Writing – original draft, Visualization, Supervision, Project administration, Methodology, Investigation, Funding acquisition, Formal analysis, Data curation, Conceptualization. **Stephen J. Jacquemin:** Writing – review & editing, Writing – original draft, Visualization, Supervision, Project administration, Methodology, Investigation, Funding acquisition, Conceptualization. **Haley E. Kuhn:** Writing – review & editing, Methodology, Investigation, Data curation. **Lillian D. Labus:** Writing – review & editing, Methodology, Investigation, Data curation. **H. Dail Laughinghouse:** Writing – review & editing, Supervision, Project administration, Methodology, Investigation, Funding acquisition, Formal analysis, Conceptualization. **Forrest W. Lefler:** Writing – review & editing, Writing – original draft, Visualization, Methodology, Investigation, Data curation. **Heath E. Mash:** Writing – review & editing, Methodology, Investigation, Data curation. **Heather A. Raymond:** Writing – review & editing, Writing – original draft, Project administration, Methodology, Investigation, Funding acquisition, Formal analysis, Data curation, Conceptualization. **Holly Stanley:** Writing – review & editing, Methodology, Investigation, Data curation. **Autumn T. Taylor:** Writing – review & editing, Methodology, Investigation, Data curation. **Linda K. Weavers:** Writing – review & editing, Writing – original draft, Visualization, Supervision, Project administration, Methodology, Investigation, Funding acquisition, Formal analysis, Data curation, Conceptualization. **Skye Wendel:** Writing – review & editing, Methodology, Investigation, Data curation.

Declaration of competing interest

The authors declare that they have no known competing financial interests or personal relationships that could have appeared to influence the work reported in this paper.

Acknowledgments

This work was funded by the United States Army Corp of Engineers' Engineer Research and Development Center, Aquatic Nuisance Species Research Program's HAB Research & Development Initiative, grant W912HZ2120013. We thank Greenwater Solutions for use of their NBOTs and flexibility in scheduling experiments; Leon Anufriyenko, Alexander Babinski, Sophia Baker, Nolan Dwenger, Madison Gels, Morgan Jutte (Grunden), Kenneth Kline, and Keara Stanislawczyk for laboratory and field assistance; the Ohio Division of Wildlife and Chris French for coordinating the delivery of GLSM water to Stone Lab; David Faler and the GLSM State Park and Theresa Dirksen and the Lake Restoration Commission for helping to facilitate site access and infrastructure. The views expressed in this article are those of the authors and do not necessarily represent the views or the policies of the U.S. Environmental Protection Agency. We thank two reviewers for their helpful comments.

Appendix A. Supplementary data

Supplementary data to this article can be found online at https://doi.org/10.1016/j.jenvman.2024.123406.

Data availability

Data from the GLSM field trip and mesocosm experiment can be found at https://github.com/justinchaffin/GLSM-NBOT-study. Sequences were deposited in the Sequence Read Archive of the National Center for Biotechnology Information (NCBI) and made publicly available under accession number PRJNA1187542. The R code used for data analysis, including a full list of R packages, is on GitHub at https://github.com/flefler/GLSM

References

Atkinson, A.J., Apul, O.G., Schneider, O., Garcia-Segura, S., Westerhoff, P., 2019. Nanobubble technologies offer opportunities to improve water treatment. Acc. Chem. Res. 52, 1196–1205. https://doi.org/10.1021/acs.accounts.8b00606.

Backer, L.C., Landsberg, J.H., Miller, M., Keel, K., Taylor, T.K., 2013. Canine cyanotoxin poisonings in the United States (1920s-2012): review of suspected and confirmed cases from three data sources. Toxins 5, 1597–1628. https://doi.org/10.3390/toxins5091597.

Bader, H., Hoigné, J., 1981. Determination of ozone in water by the indigo method. Water Res. 15, 449–456. https://doi.org/10.1016/0043-1354(81)90054-3.

Barnett, D.J. m, Arts, I.C. w, Penders, J., 2021. microViz: an R package for microbiome data visualization and statistics. J. Open Source Softw. 6, 3201. https://doi.org/10.21105/joss.03201.

Bastien, C., Cardin, R., Veilleux, É., Deblois, C., Warren, A., Laurion, I., 2011. Performance evaluation of phycocyanin probes for the monitoring of cyanobacteria. J. Environ. Monit. 13, 110–118. https://doi.org/10.1039/C0EM00366B.

Batagoda, J.H., Hewage, S.D.A., Meegoda, J.N., 2019. Nano-ozone bubbles for drinking water treatment. J. Environ. Eng. Sci. 14, 57–66. https://doi.org/10.1680/jenes.18.00015.

Beardall, J., Young, E., Roberts, S., 2001. Approaches for determining phytoplankton nutrient limitation. Aquat. Sci. 63, 44–69.

Burford, M.A., Gobler, C.J., Hamilton, D.P., Visser, P.M., Lurling, M., Codd, G.A., 2019. Solutions for Managing Cyanobacterial Blooms: A Scientific Summary for Policy Makers. UNESCO-IOC. https://doi.org/10.25607/OBP-1718 (Report).

Callahan, B.J., McMurdie, P.J., Rosen, M.J., Han, A.W., Johnson, A.J.A., Holmes, S.P., 2016. DADA2: High-resolution sample inference from Illumina amplicon data. Nat. Methods 13, 581–583. https://doi.org/10.1038/nmeth.3869.

Carmichael, W.w., 1992. Cyanobacteria secondary metabolites—the cyanotoxins. J. Appl. Bacteriol. 72, 445–459. https://doi.org/10.1111/j.1365-2672.1992.tb01858.x.

Carmichael, W.W., Boyer, G.L., 2016. Health impacts from cyanobacteria harmful algae blooms: implications for the North American great lakes. Harmful algae, global expansion of harmful cyanobacterial blooms: diversity. ecology, causes, and controls 54, 194–212. https://doi.org/10.1016/j.hal.2016.02.002.

Chaffin, J.D., Bridgeman, T.B., Bade, D.L., 2013. Nitrogen constrains the growth of late summer cyanobacterial blooms in Lake Erie. Advances in Microbiology 03 16–26. https://doi.org/10.4236/aim.2013.36A003.

Chaffin, J.D., Mishra, S., Kane, D.D., Bade, D.L., Stanislawczyk, K., Slodysko, K.N., Jones, K.W., Parker, E.M., Fox, E.L., 2019. Cyanobacterial blooms in the central basin of Lake Erie: potentials for cyanotoxins and environmental drivers. J. Great Lake. Res. 45, 277–289. https://doi.org/10.1016/j.jglr.2018.12.006.

Chang, D.-W., Hobson, P., Burch, M., Lin, T.-F., 2012. Measurement of cyanobacteria using in-vivo fluoroscopy – effect of cyanobacterial species, pigments, and colonies. Water Res. 46, 5037–5048. https://doi.org/10.1016/j.watres.2012.06.050.

City of Celina, 2022. Annual Water Quality Report: Reporting Year 2022. Online. https://celinaohio.org/wp-content/uploads/2024/02/Celina_WaterReport.pdf. (Accessed 10 November 2024).

City of Celina, 2023. Annual Water Quality Report: Reporting Year 2023. Online. https://celinaohio.org/wp-content/uploads/2024/04/CCR-2023-Web-Copy.pdf. (Accessed 10 November 2024).

Czekalski, N., Imminger, S., Salhi, E., Veljkovic, M., Kleffel, K., Drissner, D., Hammes, F., Bürgmann, H., von Gunten, U., 2016. Inactivation of antibiotic resistant bacteria and resistance genes by ozone: from laboratory experiments to full-scale wastewater treatment. Environ. Sci. Technol. 50, 11862–11871. https://doi.org/10.1021/acs.est.6b02640.

Davidson, J.L., Jacquemin, S.J., Newell, S.E., Hughes, J,C., Starr, L.D., McCarthy, M.J,. Ineffectiveness of phosphorus binding treatments in a semi-enclosed area of a large, shallow, hypereutrophic lake. Cambridge Prisms: Water. *In press*.

Djurhuus, A., Port, J., Closek, C.J., Yamahara, K.M., Romero-Maraccini, O., Walz, K.R., Goldsmith, D.B., Michisaki, R., Breitbart, M., Boehm, A.B., Chavez, F.P., 2017. Evaluation of filtration and DNA extraction methods for environmental DNA biodiversity assessments across multiple trophic levels. Front. Mar. Sci. 4. https://doi.org/10.3389/fmars.2017.00314.

Dodds, W.K., Bouska, W.W., Eitzmann, J.L., Pilger, T.J., Pitts, K.L., Riley, A.J., Schloesser, J.T., Thornbrugh, D.J., 2009. Eutrophication of U.S. freshwaters: analysis of potential economic damages. Environ. Sci. Technol. 43, 12–19. https://doi.org/10.1021/es801217q.

Dumouchelle, D.H., Stelzer, E.A., 2014. Chemical and Biological Quality of Water in Grand Lake St. Marys, Ohio, 2011–12, with Emphasis on Cyanobacteria. U.S. Geological Survey Scientific Investigations Report 2014–5210, p. 51. https://doi.org/10.3133/sir20145210.

Filbrun, J.E., Conroy, J.D., Culver, D.A., 2013. Understanding seasonal phosphorus dynamics to guide effective management of shallow, hypereutrophic Grand Lake St. Marys, Ohio. Lake Reservoir Manag. 29, 165–178. https://doi.org/10.1080/10402381.2013.823469.

Gardoni, D., Vailati, A., Canziani, R., 2012. Decay of ozone in water: a review. Ozone: Sci. Eng. 34, 233–242. https://doi.org/10.1080/01919512.2012.686354.

Golnick, P.C., Chaffin, J.D., Bridgeman, T.B., Zellner, B.C., Simons, V.E., 2016. A comparison of water sampling and analytical methods in western Lake Erie. J. Great Lake. Res. 42, 965–971. https://doi.org/10.1016/j.jglr.2016.07.031.

Gordon, G., Bubnis, B., 2002. Residual ozone measurement: indigo sensitivity coefficient adjustment. Ozone: Sci. Eng. 24, 17–28. https://doi.org/10.1080/01919510208901591.

Hazlett, L.D., Li, Q., Liu, J., McClellan, S., Du, W., Barrett, R.P., 2007. NKT cells are critical to initiate an inflammatory response after *Pseudomonas aeruginosa* ocular infection in susceptible mice. J. Immunol. 179, 1138–1146. https://doi.org/10.4049/jimmunol.179.2.1138.

He, X., Liu, Y.-L., Conklin, A., Westrick, J., Weavers, L.K., Dionysiou, D.D., Lenhart, J.J., Mouser, P.J., Szlag, D., Walker, H.W., 2016. Toxic cyanobacteria and drinking water: impacts, detection, and treatment. Harmful algae, global expansion of harmful cyanobacterial blooms. Diversity, ecology, causes, and controls 54, 174–193. https://doi.org/10.1016/j.hal.2016.01.001.

Hodges, C.M., Wood, S.A., Puddick, J., McBride, C.G., Hamilton, D.P., 2017. Sensor manufacturer, temperature, and cyanobacteria morphology affect phycocyanin fluorescence measurements. Environ. Sci. Pollut. Res. 1–10. https://doi.org/10.1007/s11356-017-0473-5.

Huang, Q., Ng, P.H., Marques, A.R.P., Cheng, T.H., Man, K.Y., Lim, K.Z., MacKinnon, B., Huang, L., Zhang, J., Jahangiri, L., Furtado, W., Hasib, F.M.Y., Zhong, L., Kam, H.Y., Lam, C.T., Liu, H., Yang, Y., Cai, W., Brettell, D., St-Hilaire, S., 2023. Effect of ozone nanobubbles on the microbial ecology of pond water and safety for jade perch (*Scortum barcoo*). Aquaculture 576, 739866. https://doi.org/10.1016/j.aquaculture.2023.739866.

ITRC (Interstate Technology & Regulatory Council), 2020. Strategies for Preventing and Managing Harmful Cyanobacterial Blooms (HCB-1). Interstate Technology & Regulatory Council, HCB Team, Washington, D.C.. www.itrcweb.org

Jacquemin, S.J., Johnson, L.T., Dirksen, T.A., McGlinch, G., 2018. Changes in water quality of Grand Lake St. Marys watershed following implementation of a distressed watershed rules package. J. Environ. Qual. 47, 113–120. https://doi.org/10.2134/jeq2017.08.0338.

Jacquemin, S.J., Birt, J., Senger, Z., Axe, B., Strang, B., Ewing, C., Kinney, B., Newell, S. E., 2023a. On the potential for reconstructed wetlands to remediate fecal coliform loading in an agricultural watershed. Hydrobiologia 850, 3879–3891. https://doi.org/10.1007/s10750-022-05078-2.

Jacquemin, S.J., Doll, J.C., Johnson, L.T., Newell, S.E., 2023b. Exploring long-term trends in microcystin toxin values associated with persistent harmful algal blooms in Grand Lake St Marys. Harmful Algae 122, 102374. https://doi.org/10.1016/j.hal.2023.102374.

Jeppesen, E., Sondergaard, M., Jensen, J.P., Havens, K.E., Anneville, O., Carvalho, L., Coveney, M.F., Deneke, R., Dokulil, M.T., Foy, B., Gerdeaux, D., Hampton, S.E., Hilt, S., Kangur, K., Kohler, J., Lammens, E.H.H.R., Lauridsen, T.L., Manca, M., Miracle, M.R., Moss, B., Noges, P., Persson, G., Phillips, G., Portielje, R., Schelske, C. L., Straile, D., Tatrai, I., Willen, E., Winder, M., 2005. Lake responses to reduced nutrient loading - an analysis of contemporary long-term data from 35 case studies. Freshw. Biol. 50, 1747–1771. https://doi.org/10.1111/j.1365-2427.2005.01415.x.

Jhunkeaw, C., Khongcharoen, N., Rungrueng, N., Sangpo, P., Panphut, W., Thapinta, A., Senapin, S., St-Hilaire, S., Dong, H.T., 2021. Ozone nanobubble treatment in freshwater effectively reduced pathogenic fish bacteria and is safe for Nile tilapia. Oreochromis niloticus). Aquaculture 534, 736286. https://doi.org/10.1016/j.aquaculture.2020.736286.

Kibuye, F.A., Zamyadi, A., Wert, E.C., 2021. A critical review on operation and performance of source water control strategies for cyanobacterial blooms: Part I-chemical control methods. Harmful Algae 109, 102099. https://doi.org/10.1016/j.hal.2021.102099.

Kinley-Baird, C., Calomeni, A., Berthold, D.E., Lefler, F.W., Barbosa, M., Rodgers, J.H., Laughinghouse, H.D., 2021. Laboratory-scale evaluation of algaecide effectiveness for control of microcystin-producing cyanobacteria from Lake Okeechobee, Florida (USA). Ecotoxicol. Environ. Saf. 207, 111233. https://doi.org/10.1016/j.ecoenv.2020.111233.

Kuhn, H.E., 2024. Use of a Modified Indigo Method to Quantify Ozone Diffusion from Nanobubbles. Master's thesis. Ohio State University.

Laughinghouse IV, H.D., Altarugio, J.M., Berthold, D.E., Lefler, F.W., 2024. Effects of nanobubble oxygenated water technologies on managing water quality, microbial community structure and cyanobacterial harmful algal blooms. https://www.ggefound.org/assets/docs/UF%20GGEF_finalreport.pdf.

Lee, Y., Gerrity, D., Lee, M., Bogeat, A.E., Salhi, E., Gamage, S., Trenholm, R.A., Wert, E. C., Snyder, S.A., von Gunten, U., 2013. Prediction of micropollutant elimination during ozonation of municipal wastewater effluents: use of kinetic and water specific information. Environ. Sci. Technol. 47, 5872–5881. https://doi.org/10.1021/es400781r.

Lefler, F.W., Berthold, D.E., Barbosa, M., Laughinghouse, H.D., 2022. The effects of algaecides and herbicides on a nuisance *Microcystis wesenbergii*-dominated bloom. Water 14, 1739. https://doi.org/10.3390/w14111739.

Lefler, F.W., Berthold, D.E., Laughinghouse IV, H.D., 2023. Cyanoseq: a database of cyanobacterial 16S rRNA gene sequences with curated taxonomy. J. Phycol. 59, 470–480. https://doi.org/10.1111/jpy.13335.

Matthijs, H.C.P., Visser, P.M., Reeze, B., Meeuse, J., Slot, P.C., Wijn, G., Talens, R., Huisman, J., 2012. Selective suppression of harmful cyanobacteria in an entire lake with hydrogen peroxide. Water Research, Cyanobacteria: impacts of climate change on occurrence. toxicity and water quality management 46, 1460–1472. https://doi.org/10.1016/j.watres.2011.11.016.

McMurdie, P.J., Holmes, S., 2013. phyloseq: an R package for reproducible interactive analysis and graphics of microbiome census data. PLoS One 8, e61217. https://doi.org/10.1371/journal.pone.0061217.

Meegoda, J.N., Hewage, S.A., Batagoda, J.H., 2019. Application of the diffused double layer theory to nanobubbles. Langmuir 35, 12100–12112. https://doi.org/10.1021/acs.langmuir.9b01443.

Mishra, S., Stumpf, R.P., Schaeffer, B.A., Werdell, P.J., Loftin, K.A., Meredith, A., 2019. Measurement of cyanobacterial bloom magnitude using satellite remote sensing. Sci. Rep. 9, 1–17.

Morrison, C.M., Hogard, S., Pearce, R., Mohan, A., Pisarenko, A.N., Dickenson, E.R.V., von Gunten, U., Wert, E.C., 2023. Critical review on bromate formation during ozonation and control options for its minimization. Environ. Sci. Technol. 57, 18393–18409. https://doi.org/10.1021/acs.est.3c00538.

Newell, S.E., Doll, J.C., Jutte, M.C., Davidson, J.L., McCarthy, M.J., Jacquemin, S.J., 2024. Drivers and mechanisms of harmful algal blooms across hydrologic extremes in hypereutrophic Grand Lake St Marys (Ohio). Harmful Algae 102684. https://doi.org/10.1016/j.hal.2024.102684.

Nogaro, G., Burgin, A.J., Schoepfer, V.A., Konkler, M.J., Bowman, K.L., Hammerschmidt, C.R., 2013. Aluminum sulfate (alum) application interactions with coupled metal and nutrient cycling in a hypereutrophic lake ecosystem. Environmental Pollution 176, 267–274. https://doi.org/10.1016/j.envpol.2013.01.048.

Ohio EPA, 2020. Application of aquatic pesticides and algaecides to reservoirs used as a public drinking water supply. Ohio EPA, Division of Surface Water and Division of Drinking and Ground Waters, May 2020. Columbus, OH. https://dam.assets.ohio.gov/image/upload/epa.ohio.gov/Portals/28/documents/habs/Publications/AlgaecideApplicationFactSheet.pdf.

Ohio EPA, 2021. Ohio EPA total (extracellular and intracellular) microcystins-ADDA by ELISA analytical methodology. Ohio EPA Method 701.0. Version 2.4. https://dam.assets.ohio.gov/image/upload/epa.ohio.gov/Portals/28/documents/labcert/Microcystin-SOP.pdf.

Ohio EPA, 2024. Drinking water watch, city of Celina bromate results. Online Access 10/11/2024. https://dww.epa.ohio.gov/DWW/JSP/NonTcrSamples.jsp?tinwsys_is_number=4388&tinwsys_st_code=OH&tsaanlyt_is_number=728&tsaanlyt_st_code=HQ&history=1&counter=0.

Oksanen, J., Simpson, G., Blanchet, F., Kindt, R., Legendre, P., Minchin, P., O'Hara, R., Solymos, P., Stevens, M., Szoecs, E., Wagner, H., Barbour, M., Bedward, M., Bolker, B., Borcard, D., Carvalho, G., Chirico, M., De Caceres, M., Durand, S., Evangelista, H., FitzJohn, R., Friendly, M., Furneaux, B., Hannigan, G., Hill, M., Lahti, L., McGlinn, D., Ouellette, M., Ribeiro Cunha, E., Smith, T., Stier, A., Ter Braak, C., Weedon, J., 2024. Vegan: community ecology package. R package version 2, 6–7. https://github.com/vegandevs/vegan. https://vegandevs.github.io/vegan/.

Osgood, D., Gibbons, H., Brattebo, S., 2017. Lake Management Best Practices: Alum for Phosphorus Control in Lakes and Ponds. Lake Advocates Publishers, Duluth, Minnesota, USA.

Osterholz, W.R., Hanrahan, B.R., King, K.W., 2020. Legacy phosphorus concentration–discharge relationships in surface runoff and tile drainage from Ohio crop fields. J. Environ. Qual. 49, 675–687. https://doi.org/10.1002/jeq2.20070.

O'Neil, J.M., Davis, T.W., Burford, M.A., Gobler, C.J., 2012. The rise of harmful cyanobacteria blooms: the potential roles of eutrophication and climate change. Harmful Algae, Harmful Algae–The requirement for species-specific information 14, 313–334. https://doi.org/10.1016/j.hal.2011.10.027.

Paerl, H.W., Huisman, J., 2008. Blooms like it hot. Science 320, 57–58. https://doi.org/10.1126/science.1155398.

Parada, A.E., Needham, D.M., Fuhrman, J.A., 2016. Every base matters: assessing small subunit rRNA primers for marine microbiomes with mock communities, time series and global field samples. Environ. Microbiol. 18, 1403–1414. https://doi.org/10.1111/1462-2920.13023.

Patton, C.J., Kryskalla, J.R., 2003. Methods of Analysis by the U.S. Geological Survey National Water Quality Laboratory-Evaluation of Alkaline Persulfate Digestion as an Alternative to Kjeldahl Digestion for Determination of Total and Dissolved Nitrogen and Phosphorus in Water. USGS.

Peterson, E.S., Summers, R.S., 2021. Removal of effluent organic matter with biofiltration for potable reuse: a review and meta-analysis. Water Res. 199, 117180. https://doi.org/10.1016/j.watres.2021.117180.

Plaas, H.E., Paerl, H.W., 2021. Toxic cyanobacteria: a growing threat to water and air quality. Environ. Sci. Technol. 55, 44–64. https://doi.org/10.1021/acs.est.0c06653.

Qin, B., Zhu, G., Gao, G., Zhang, Y., Li, W., Paerl, H.W., Carmichael, W.W., 2010. A drinking water crisis in Lake Taihu, China: linkage to climatic variability and lake management. Environ Manage 45, 105–112. https://doi.org/10.1007/s00267-009-9393-6.

Quast, C., Pruesse, E., Yilmaz, P., Gerken, J., Schweer, T., Yarza, P., Peplies, J., Glöckner, F.O., 2013. The SILVA ribosomal RNA gene database project: improved data processing and web-based tools. Nucleic Acids Res. 41, D590–D596. https://doi.org/10.1093/nar/gks1219.

Rakness, K.L., 2011. Ozone in Drinking Water Treatment: Process Design, Operation, and Optimization. American Water Works Association.

Richard, Y., 1994. Ozone water demand test. Ozone: Sci. Eng. 16, 355–365. https://doi.org/10.1080/01919519408552320.

Rositano, J., Nicholson, B.C., Pieronne, P., 1998. Destruction of cyanobacterial toxins by ozone. Ozone: Sci. Eng. 20, 223–238. https://doi.org/10.1080/01919519808547273.

Schloss, P.D., 2023. Waste not, want not: revisiting the analysis that called into question the practice of rarefaction. mSphere 9, e00355. https://doi.org/10.1128/msphere.00355-23, 23.

Shawwa, A.R., Smith, D.W., 2001. Kinetics of microcystin-LR oxidation by ozone. Ozone: Sci. Eng. 23, 161–170. https://doi.org/10.1080/01919510108961998.

Shi, J.H., Olson, N.E., Birbeck, J.A., Pan, J., Peraino, N.J., Holen, A.L., Ledsky, I.R., Jacquemin, S.J., Marr, L.C., Schmale, D.G.I., Westrick, J.A., Ault, A.P., 2023. Aerosolized cyanobacterial harmful algal bloom toxins: microcystin congeners quantified in the atmosphere. Environ. Sci. Technol. 57, 21801–21814. https://doi.org/10.1021/acs.est.3c03297.

Shoemaker, J., Tettenhorst, D., Delacruz, A., 2015. Method 544. Determination of Microcystins and Nodularin in Drinking Water by Solid Phase Extraction and Liquid Chromatography/tandem Mass Spectrometry (LC/MS/MS). U.S. Environmental Protection Agency, Washington, DC, 2015.

Smith, R.B., Bass, B., Sawyer, D., Depew, D., Watson, S.B., 2019. Estimating the economic costs of algal blooms in the Canadian Lake Erie Basin. Harmful Algae 87, 101624. https://doi.org/10.1016/j.hal.2019.101624.

Søndergaard, M., Jensen, J.P., Jeppesen, E., 2003. Role of sediment and internal loading of phosphorus in shallow lakes. Hydrobiologia 506, 135–145.

Soyluoglu, M., Kim, D., Karanfil, T., 2023. Characteristics and stability of ozone nanobubbles in freshwater conditions. Environ. Sci. Technol. 57, 21898–21907. https://doi.org/10.1021/acs.est.3c07443.

Steffen, M.M., Davis, T.W., McKay, R.M.L., Bullerjahn, G.S., Krausfeldt, L.E., Stough, J.M. A., Neitzey, M.L., Gilbert, N.E., Boyer, G.L., Johengen, T.H., Gossiaux, D.C., Burtner, A.M., Palladino, D., Rowe, M.D., Dick, G.J., Meyer, K.A., Levy, S., Boone, B. E., Stumpf, R.P., Wynne, T.T., Zimba, P.V., Gutierrez, D., Wilhelm, S.W., 2017. Ecophysiological examination of the Lake Erie *Microcystis* bloom in 2014: linkages between biology and the water supply shutdown of Toledo, OH. Environ. Sci. Technol. 51, 6745–6755. https://doi.org/10.1021/acs.est.7b00856.

Sukenik, A., Kaplan, A., 2021. Cyanobacterial harmful algal blooms in aquatic ecosystems: a comprehensive outlook on current and emerging mitigation and control approaches. Microorganisms 9, 1472. https://doi.org/10.3390/microorganisms9071472.

Thanh Dien, L., Linh, N.V., Sangpo, P., Senapin, S., St-Hilaire, S., Rodkhum, C., Dong, H. T., 2021. Ozone nanobubble treatments improve survivability of Nile tilapia (*Oreochromis niloticus*) challenged with a pathogenic multi-drug-resistant Aeromonas hydrophila. J. Fish. Dis. 44, 1435–1447. https://doi.org/10.1111/jfd.13451.

Tillmanns, A.R., Wilson, A.E., Pick, F.R., Sarnelle, O., 2008. Meta-analysis of cyanobacterial effects on zooplankton population growth rate: species-specific responses. Fundamental and Applied Limnology/Arch. Hydrobiol. 171, 285–295. https://doi.org/10.1127/1863-9135/2008/0171-0285.

Tsai, K.-P., Kirschman, Z.A., Moldaenke, C., Chaffin, J.D., McClure, A., Seo, Y., Bridgeman, T.B., 2024. Field and laboratory studies of fluorescence-based technologies for real-time tracking of cyanobacterial cell lysis and potential microcystins release. Sci. Total Environ. 920, 171121. https://doi.org/10.1016/j.scitotenv.2024.171121.

US EPA, 2015. Recommendations for Public Water Systems to Manage Cyanotoxins in Drinking Water. USEPA, Office of Water (4606M), EPA 815-R-15-010, June 2015.
Verspagen, J.M.H., Van de Waal, D.B., Finke, J.F., Visser, P.M., Van Donk, E., Huisman, J., 2014. Rising CO2 levels will intensify phytoplankton blooms in eutrophic and hypertrophic lakes. PLoS One 9, e104325. https://doi.org/10.1371/journal.pone.0104325.
von Gunten, U., Pinkernell, U., 2000. Ozonation of bromide-containing drinking waters:a delicate balance between disinfection and bromate formation. Water Sci. Technol. 41, 53–59. https://doi.org/10.2166/wst.2000.0115.
Wang, Q., Garrity, G.M., Tiedje, J.M., Cole, J.R., 2007. Naïve Bayesian classifier for rapid assignment of rRNA sequences into the new bacterial taxonomy. Appl. Environ. Microbiol. 73, 5261–5267. https://doi.org/10.1128/AEM.00062-07.
Waters, S., Hamilton, D., Pan, G., Michener, S., Ogilvie, S., 2022. Oxygen nanobubbles for lake restoration—where are we at? A review of a new-generation approach to managing lake eutrophication. Water 14, 1989. https://doi.org/10.3390/w14131989.
Weishaar, J.L., Aiken, G.R., Bergamaschi, B.A., Fram, M.S., Fujii, R., Mopper, K., 2003. Evaluation of specific ultraviolet absorbance as an indicator of the chemical composition and reactivity of dissolved organic carbon. Environ. Sci. Technol. 37, 4702–4708. https://doi.org/10.1021/es030360x.
Wickham, H., 2016. ggplot2: Elegant Graphics for Data Analysis. Use R! Springer International Publishing, Cham. https://doi.org/10.1007/978-3-319-24277-4.
Wolf, C., Pavese, A., von Gunten, U., Kohn, T., 2019. Proxies to monitor the inactivation of viruses by ozone in surface water and wastewater effluent. Water Res. 166, 115088. https://doi.org/10.1016/j.watres.2019.115088.
Wolf, D., Gopalakrishnan, S., Klaiber, H.A., 2022. Staying afloat: the effect of algae contamination on Lake Erie housing prices. Am. J. Agric. Econ. 104, 1701–1723. https://doi.org/10.1111/ajae.12285.
World Health Organization, 2020. Cyanobacterial Toxins: Microcystins. Background Document for Development of WHO Guidelines for Drinking-Water Quality and Guidelines for Safe Recreational Water Environments.
Zepernick, B.N., Wilhelm, S.W., Bullerjahn, G.S., Paerl, H.W., 2023. Climate change and the aquatic continuum: a cyanobacterial comeback story. Environmental Microbiology Reports 15, 3–12. https://doi.org/10.1111/1758-2229.13122.